Title
Model Reduction and Parameter Estimation in Groundwater Modeling

Author
Siade, Adam

Publication Date
2012

Peer reviewed|Thesis/dissertation

University of California

Los Angeles

Model Reduction and Parameter Estimation in Groundwater Modeling

A dissertation submitted in partial satisfaction

of the requirements for the degree

Doctor of Philosophy in Civil Engineering

by

Adam John Siade

2012

ABSTRACT OF THE DISSERTATION

Model Reduction and Parameter Estimation in Groundwater Modeling

by

Adam John Siade
Doctor of Philosophy in Civil Engineering
University of California, Los Angeles, 2012
Professor William W-G. Yeh, Chair

Water resources systems management often requires complex mathematical models whose use may be computationally infeasible for many advanced analyses. The computational demand of these analyses can be reduced by approximating the model with a simpler reduced model. Proper Orthogonal Decomposition (POD) is an efficient model reduction technique based on the projection of the original model onto a subspace generated by full-model snapshots. In order to implement this method, an appropriate number of snapshots of the full model must be taken at the appropriate times such that the resulting reduced model is as accurate as possible. Since confined aquifers reach steady state in an exponential manner, a simple exponential function can be used to select snapshots for these types of models. This selection method is then employed to determine the optimal snapshot set for a unit, dimensionless model. The optimal snapshot set is found by maximizing the minimum eigenvalue of the snapshot covariance matrix, a criterion similar to those used in experimental design. The resulting snapshot set can then be translated to any complex, real world model based on a simple, approximate relationship between dimensionless and real-world times. This translation is illustrated using a basin scale model of Central Veneto, Italy, where the reduced model runs approximately 1,000 times faster than the full model. Accurate reduced

modeling can be significantly beneficial for advanced analyses such as parameter estimation. A new parameter estimation algorithm is proposed that is an extension of the quasilinearization approach where the governing system of differential equations is linearized with respect to the parameters. The resulting inverse problem therefore becomes a quadratic programming problem (QP) for minimizing the sum of squared residuals; the solution becomes an update on the parameter set. This process of linearization and regression is repeated until convergence takes place. POD is applied to reduce the size of the linearized model, thereby reducing the computational burden of solving each QP. In fact, this study shows that the snapshots need only be calculated once at the very beginning of the algorithm, after which no further calculations of the reduced-model subspace are required. The proposed algorithm therefore only requires one linearized full-model run per parameter at the first iteration followed by a series of reduced-order QPs. The method is applied to a groundwater model with about 30,000 computation nodes where as many as 15 zones of hydraulic conductivity are estimated.

The dissertation of Adam John Siade is approved.

Mario Putti

Terri Hogue

Steve Margulis

Weng Kee Wong

William W-G. Yeh, Committee Chair

University of California, Los Angeles

2012

Contents

List of Figures

List of Tables

VITA

1978	Born, Valparaiso, Indiana
2006	B.S., Environmental Resources Engineering, Humboldt State University, Arcata, California
2006	Engineering Graduate of the Year Award, Environmental Resources Engineering, Humboldt State University, Arcata, California
2007	M.S., Civil and Environmental Engineering, University of California, Los Angeles Los Angeles, Californi
2007 – present	Engineering Graduate of the Year Award, Environmental Resources Engineering, Humboldt State University, Arcata, California

PUBLICATIONS AND PRESENTATIONS

Nishikawa, T., Siade, A. J., Reichard, E. G., Ponti, D. J., Canales, A. G., and Johnson, T. A. (2009), Stratigraphic controls on seawater intrusion and implications for groundwater management, Dominguez Gap are of Los Angeles, California, USA, *Hydrogeology Journal*, 17, 1699-1725.

Siade, A. J., M. Putti, and W. W.-G. Yeh (2010), Snapshot selection for groundwater model reduction using proper orthogonal decomposition, *Water Resour. Res.*, 46, W08539, doi:10.1029/2009WR008792.

Siade, A. J., M. Putti, and W. W.-G. Yeh (2012), Reduced order parameter estimation using quasilinearization and quadratic programming, *Water Resour. Res.*, submitted Sept., 2011

Siade, A. J., Nishikawa, T., Reichard, E. G., Ponti, D. J., Canales, A. G., and Johnson, T. A. (2007), Stratigraphic controls on seawater intrusion and implications for groundwater management, Dominguez Gap are of Los Angeles, California, USA. American Geophysical Union Fall Meeting, San Francisco, California, USA.

Siade, A. J., Kendall, D., Putti, M., and Yeh, W. W-G. (2008), Model reduction in groundwater modeling and management. American Geophysical Union Fall Meeting, San Francisco, California, USA.

Siade, A. J., Putti, M., Kendall, D., and Yeh, W. W-G. (2009), Reduced order parameter estimation using quasilinearization and quadratic programming. American Geophysical Union Fall Meeting, San Francisco, California, USA.

Siade, A. J., Cheng, W-C., and Yeh, W. W-G. (2010), Experimental design for groundwater pumping estimation using genetic algorithm and proper orthogonal decomposition. American Geophysical Union Fall Meeting, San Francisco, California, USA.

Siade, A. J., Nishikawa, T., and Martin, P. (2011). The progression of studies by the U.S. Geological Survey to improve the understanding of the aquifer system in Antelope Valley, California, USA: from artesian to adjudication. 28^{th} Biennial Groundwater Conference and 20^{th} Groundwater Resources Association Annual Meeting, Sacramento, California, USA.

Siade, A. J., Nishikawa, T., and Martin, P. (2011). Natural recharge estimation and uncertainty analysis of an adjudicated groundwater basin using a regional-scale groundwater flow and subsidence model. American Geophysical Union Fall Meeting, San Francisco, California, USA.

Chapter 1

Introduction

Groundwater management requires the development and implementation of mathematical models that, through simulation, evaluate the anthropogenic impacts on an aquifer system. These models must exhibit a significant degree of accuracy in order to provide reliable results that can be used for prediction and management purposes. The accuracy and reliability of a model is predicated on many factors including the quality and quantity of observed data, the complexity of the model parameterization, and correct identification of model parameters and initial and boundary conditions. There are many well developed methods for dealing with these factors; however, computing power limits some of them. For example, a groundwater model with a coarse spatial discretization will yield inaccurate results, yet a model with too fine of a discretization will require so much computer time that its use may be impractical.

Highly heterogeneous groundwater models require a degree of model complexity that corresponds to that of the subsurface lithology. In other words, aquifers whose properties change significantly within a certain distance are best represented using a model with a discretization on that same order of magnitude. However, matching the model discretization with the complexity of the aquifer can be impractical due to computational demand. Therefore, there exists a trade-off between accuracy and model computation time. Even

though current computing technology affords the use of complex models, there are many cases where forward simulation is still inefficient. Even though a single forward simulation of a groundwater model may seem effective, the computational expense resides in the need to call the model numerous times depending on the analysis under consideration e.g., parameter identification, management/optimization, data assimilation, and model uncertainty analysis [18].

There exist a multitude of techniques designed to alleviate the computational demand required of a numerical model. These techniques are known as model reduction techniques where the objective is to develop a reduced model with a much smaller dimension for fast execution. The reduced model is of course only an approximation of the full model and the introduced model error must be closely examined. Model reduction can be classified into three major categories: data driven, model driven and combined methods. Data driven methods assume a black box model where the objective is only to match inputs with their respective outputs. Model driven methods make use of the mathematical structure of the model itself when developing the reduced model. Combined methods make use of input/output data relationships as well as incorporate the physics of the model.

Artificial neural networks (ANNs) are an example of data driven methods. In this approach, the response of a full model is simulated explicitly by an ANN model based on biological neural networks, which is much easier and faster to execute. A number of full model simulations are conducted to generate an input and output data set, which is then used to train a black box model. *Rogers and Dowla* [31] used an ANN model to replace a groundwater flow and contaminant transport model in a management scenario in which the objective was to prevent migration of a contaminant plume. However, in order to train the ANN model, numerous calls to the full model must be evaluated to provide enough data for an accurate surrogate model. *Yan and Minsker* [42] developed a methodology for reducing the number of full-model calls using a dynamic learning technique. A technique similar to

ANN modeling is a method proposed by *Baú and Mayer* [2] in which the objective functions are approximated using kriging interpolation, resulting in surrogate functions which reduce the computational burden of the management problem presented in their work.

Inverse eigenvalue methods are an example of model driven methods designed to exploit the mathematical structure of the full model. The full numerical model often involves large, general matrices. The inverse eigenvalue approach projects the model onto a subspace by finding smaller matrices that share the same nonzero/significant eigenvalue spectrum as their corresponding full-model matrices. The reader is referred to *Chu* [12] for a complete introduction to inverse eigenvalue problems. *Orbak et al.* [1] evaluated the sensitivities of the system parameters with respect to eigenvalues for some simple example problems. "Effect" matrices were then developed allowing for physical model reduction via inverse eigenvalue methods.

The third category of model reduction combines concepts from both the data and model driven methods. The distribution of the state variables is sampled from the full model for various values of the decision variables and time. These samples are called snapshots of the full model and are used in an interpolation scheme to approximate the full model. The act of interpolating reduces the dimensionality of the problem allowing for model reduction. This is equivalent to considering only a subspace of the vector space where the full-model solution resides. This subspace is evaluated so that it captures the majority of the variation in the model solution. The entire model is then projected onto this subspace and solved, resulting in a fast approximate solution to the original model. Depending on the application, the method in which the spatial patterns (basis functions that define the reduced model space) are developed has been called Proper Orthogonal Decomposition (POD) [10, 40], Principal Component Analysis (PCA) or the discrete Karhunen Lòeve Transform [23, 49]. The spatial basis functions have been called Principal Vectors, Empirical Orthogonal Functions (EOFs) [39, 25], or Coherent Structures (CS) [26].

The focus of this study is on the efficient development of combined model reduction methods for groundwater flow models. *Vermeulen et al.* [39] and *McPhee and Yeh* [25] developed reduced groundwater models by sampling hydraulic head distributions for some constant, reference pumping rate at specified time intervals. These snapshots were then used to determine the EOFs of the system. The evaluation of these snapshots, a phase shared by all combined model reduction methods, requires one full-model run per stress location (pumping/injection well) from early times to steady state. However, there is no established method for determining a best snapshot selection scheme, *i.e.*, at which time steps the full-model solution is to be recorded and used to develop the reduced model. The optimal selection strategy would yield the smallest set of full-model state variable snapshots such that the resulting reduced-model solution achieves a predefined accuracy. However, in order to optimally select snapshots, the dynamics of the system must be well understood [39, 25]. Once a good snapshot set is obtained, the model can be reduced via POD and time-varying extraction rates can be applied to the reduced model, *i.e.*, the superposition principle applies due to the linearity of the governing equations.

Snapshot selection for POD model reduction has received little attention and requires further research. *Kowalski and Jin* [20] performed POD model reduction for Maxwells equations, used to model the performance of a medical device in the human body. They considered three snapshot selection techniques: uniform in time, logarithmic with a focus on early time steps and logarithmic with a focus on later time steps. The early-time logarithmic selection scheme produced the best results. They concluded that the optimal snapshot selection scheme depends on the mathematical model under investigation and the parametric structure of that model. The objective of the second chapter of this dissertation is to conduct POD model reduction for confined groundwater aquifers and to develop a strategy for snapshot selection based on both the governing equation and the parametric structure of the model.

As previously mentioned, a significant advantage associated with reducing the forward

run time of a numerical model resides in the need to run the model many times. This need arises in advanced analyses such as parameter identification, management/optimization, data assimilation, predictive uncertainty analysis, etc. The third chapter of this dissertation focuses on the application of model reduction techniques in the field of parameter identification.

In order for a groundwater flow model to accurately simulate the response of a real world aquifer, intrinsic model parameters and their structure must be identified. A multitude of algorithms exist whose purpose is to adjust the parameter values of a model such that the model output matches its associated measured values as closely as possible. This type of problem is commonly referred to as the inverse problem. *Yeh* [44], *Sun* [33] and *Oliver and Chen* [27] provide comprehensive reviews on the inverse problem as it applies to groundwater hydrology. Currently, the most popular methods are based on the output error criterion, where a starting estimate of the parameter vector is updated such that the norm of the difference between observed states and their corresponding model predicted values is minimized. Methods based on the output error criterion require a significant number of model runs in order to evaluate parameter updates from one iteration to the next. Therefore, the computational demand associated with a forward run of the numerical model has a large impact on the overall CPU requirement of the parameter estimation algorithm. *Cooley* [14] provides a comparison of four different nonlinear regression methods of parameter identification; the most efficient methods were found to be the Marquardt [24] and quasilinearization [47, 46] methods. Some current, popular software include PEST [15] and UCODE [30]. These software applications employ algorithms that are largely based on Gauss-Marquardt-Levenberg methods [24, 21].

The application of the POD model reduction technique can significantly reduce the computational expense associated with parameter identification. However, the accuracy of the reduced model via POD is dependent on the quality of the basis functions that span the reduced model subspace. When the objective is to change the values of the parameters, such

as hydraulic conductivity, these basis functions can begin to lose accuracy. This loss of accuracy is due to the nonlinear relationship between model parameters and model states. This presents a problem for reduced-order parameter estimation, which requires iterative updates of the parameter values. *Park et al.* [28] and *Vermeulen et al.* [38] present methodologies for dealing with this issue. In both articles, the authors use the method of snapshots to develop the basis functions that span the reduced model space. A snapshot set is collected for each well, individually, given a constant unit forcing and a specific set of parameter values. Snapshot sets are collected over a specific range of parameter values that adequately capture parameter variability around their current estimates. Throughout the parameter estimation algorithm, the current estimate of the parameters may "travel" outside this range, requiring the re-evaluation of the reduced model using a new range of parameter values. However, many snapshot sets are needed in order to adequately capture all possible combinations of parameter ranges each time the reduced model is evaluated. For example, a snapshot set for each extraction/injection well is needed when one of the parameters is at the upper end of its range and the others are at their lower ends. Additional snapshot sets are required for each of these combinations at each extraction/injection well. In particular, in the case of one well and two parameters, four snapshot sets are needed; in the case of two wells and three parameters, 16 snapshot sets are needed, etc. Additionally, snapshot sets may be required for parameter values within their ranges rather than at the upper and lower bounds only. Each snapshot set requires an original full-model run. Therefore, for highly parameterized systems with a large number of extraction wells, the computational gain of the model reduction is overcome by the computational burden of developing snapshot sets.

In this dissertation, a new methodology is proposed that no longer requires the development of a "moving" parameter range when developing snapshots. The reduced model must be developed once only; the resulting basis functions are accurate for the entire parameter estimation procedure. The parameters under investigation are zonal hydraulic conductivity

values. The parameter estimation procedure employed is based on quasilinearization and quadratic programming. *Bellman and Kalaba* [5] originally developed quasilinearization for parameter identification in a system of nonlinear ordinary differential equations. It involves solving a series of linearized initial value problems such that the sequence of solutions converges to the solution of the original nonlinear problem. *Yeh and Tauxe* [47, 46] applied quasilinearization to parameter estimation in groundwater modeling while *Park et al* [28] applied it to flow reactor modeling. *Yeh* [43] combined quasilinearization and quadratic programming for parameter estimation in a partial differential equation. The algorithm essentially consisted of solving a series of sequential quadratic programming (QP) problems. However, in practice this algorithm suffers from the fact that each QP problem is so large that the computational burden of solving it is near the same magnitude as that of current Gauss-Newton type approaches. In the research presented in this dissertation, it is shown that POD model reduction can dramatically reduce the computational requirement of the individual QP problems, resulting in a drastic increase in overall inversion efficiency. The method requires the evaluation of one snapshot set for each hydraulic conductivity zone in order to build the reduced model. Snapshots are collected from the linearized full model (where changes in conductivity become the forcing term) rather than the original full model (where groundwater extraction/injection is the forcing term). The proposed method can handle highly parameterized systems with a large number of extraction/injection wells and still achieve significant reductions in CPU time.

Chapter 2

Snapshot Selection for Groundwater Model Reduction using Proper Orthogonal Decomposition

2.1 Confined Aquifer Groundwater Flow Model

The following partial differential equation (PDE) describes threedimensional groundwater flow for a confined, anisotropic aquifer with pumping [3],

$$\frac{\partial}{\partial x}\left(K_x\frac{\partial h}{\partial x}\right)+\frac{\partial}{\partial y}\left(K_y\frac{\partial h}{\partial y}\right)+\frac{\partial}{\partial z}\left(K_z\frac{\partial h}{\partial z}\right)-q-S_s\frac{\partial h}{\partial t}=0, \tag{2.1}$$

with initial and boundary conditions:

$$\begin{aligned} h(x,y,z,0) &= f_1(x,y,z); \\ h(x,y,z,t) &= f_2(x,y,z,t),\ (x,y,z,t)\in(\Gamma_1); \\ q_n(x,y,z,t) &= f_3(x,y,z,t),\ (x,y,z,t)\in(\Gamma_2); \end{aligned} \tag{2.2}$$

where h is the hydraulic head (L), K_x, K_y, K_z are hydraulic conductivities in the $x-$, $y-$, and $z-$directions, respectively (L/T), S_s is the specific storage (L^{-1}), q is the specific volumetric pumping rate (T^{-1}), q_n is the specific discharge normal to the flux boundary Γ_2 (T^{-1}), Γ_1 is the fixed head boundary, f_1, f_2 and f_3 are known functions.

Application of the superposition principle followed by spatial discretization of the resulting PDE (*e.g.*, by finite differences, finite elements, etc.) yields a system of linear ordinary differential equations (ODEs) for the drawdown:

$$\mathbf{B}\frac{d\mathbf{s}}{dt} + \mathbf{A}\mathbf{s} = \mathbf{q} \tag{2.3}$$

where $\mathbf{A}$ is the $n \times n$ stiffness matrix, $\mathbf{B}$ is the $n \times n$ mass matrix, $\mathbf{s}$ and $\mathbf{q}$ are the $n-$dimensional vectors of nodal (cell) drawdowns and sinks, respectively, and n is the number of spatial computational nodes (cells), which is generally very large. Drawdown is the difference between the initial head and the head after pumping, *i.e.*, $s = H - h$, where H is the initial head (*e.g.*, steady state or the natural system dynamics). In the majority of cases of practical interest, matrices $\mathbf{A}$ and $\mathbf{B}$ are large, sparse, symmetric and positive definite.

2.2 Model Reduction via Proper Orthogonal Decomposition

In this section, a summary of the method of POD model reduction is provided. This summary is a culmination of many previous works, including those by *Cazemier et al.* [10], *Willcox and Peraire* [40], *Kowalski and Jin* [20], *Vermeulen et al.* [39], and *McPhee and Yeh* [25].

2.2.1 Subspace Projection

Model reduction via POD is achieved by projecting the state vector into an n_p-dimensional subspace ($n_p \ll n$) such that $\hat{\mathbf{s}} = \mathbf{P}\mathbf{s}_r$, where $\hat{\mathbf{s}} \in \mathbb{R}^n$ is an approximation of the state vector after subspace projection, $\mathbf{P}$ is a projection operator represented by a matrix whose columns form an orthonormal basis spanning the subspace $V \subset \mathbb{R}^n$, and $\mathbf{s}_r \in \mathbb{R}^{n_p}$ is the state vector of the reduced model. This can also be written as follows [39]:

$$\hat{\mathbf{s}} = \mathbf{s}_{nat}(t) + \sum_{k=1}^{n_p} \mathbf{p}_k s_{r_k}(t) \tag{2.4}$$

where, $\mathbf{s}_{nat}(t)$ is the natural system dynamics without forcing (*e.g.*, the steady state solution) and s_{r_k} indicates the k-th component of $\mathbf{s}_r$. Note here that generally, $\mathbf{s}_{nat}(t) = 0$.

The definition of the n_p basis vectors that span the subspace V proceeds by selecting from a full-model model run n_s numerical solution vectors (snapshots) at predefined times. This must be done for each well individually with constant pumping rates. These snapshots (here identified by the $n-$dimensional vectors $\mathbf{s}_i$, $i = 1, \ldots, n_s$) must be significantly different and cover the overall range or variability of the full model. Note that $n_s \geq n_p$ where n_s is often much greater than n_p. The basis vectors for V are then obtained via PCA as follows. Once the snapshots have been taken, the so called covariance matrix [32] can be calculated as $\mathbf{C} = \mathbf{X}\mathbf{X}^T$, where $\mathbf{X} = \{\bar{\mathbf{s}}_1, \ldots, \bar{\mathbf{s}}_{n_s}\}$ and $\bar{\mathbf{s}}_i$ is the $i-$th normalized snapshot [25, 39]. From PCA, the eigenvectors (or principal vectors) $\mathbf{p}_k$ of $\mathbf{C}$ are linearly independent and mutually orthogonal. These principal vectors can be considered as candidates for the spatial basis functions that are used to express the problem solution in the reduced space.

In practice, the length of each snapshot vector is large, as it is equal to the number of nodes in the model; this will cause the eigenvalue decomposition of the resulting $\mathbf{C}$ matrix to be computationally infeasible. This is remedied by calculating the eigenpairs of $\mathbf{C}_s = \mathbf{X}^T\mathbf{X}$, that are related to the eigenpairs of $\mathbf{C}$. It is easy to prove, in fact, that if $(\lambda_k, \mathbf{g}_k)$ is the

$k-$th eigenpair of $\mathbf{C}_s$, then $\lambda_k, \mathbf{u}_k = \mathbf{X}\mathbf{g}_k$ characterizes the eigenpair of $\mathbf{C}$ corresponding to the $k-$th nonzero eigenvalue.

Once the eigenvalues of $\mathbf{C}$ are calculated, insignificant principal vectors can be removed from the basis for further subspace dimension reduction. This is accomplished by normalizing the eigenvalues to represent relative magnitudes as follows:

$$\phi_j = \frac{\lambda_j}{\sum_{i=1}^{n_s} \lambda_i} \tag{2.5}$$

The largest n_p normalized eigenvalues and their corresponding eigenvectors are retained for use in the reduced model and the rest are discarded. The parameter n_p is chosen such that $\sum_{i=1}^{n_p} \geq \Phi$ where Φ is user-specified [25]. Finally, imposing $\mathbf{P}^T\mathbf{P} = \mathbf{I}$, the matrix of the basis vectors for V is calculated as

$$\mathbf{P} = \mathbf{X}\mathbf{G}\Lambda^{-1/2} \tag{2.6}$$

where $\mathbf{G}$ and Λ are the rectangular and diagonal matrices that consist of the n_p retained eigenvectors, $\mathbf{g}_k$, and the corresponding eigenvalues, λ_k, respectively.

In other words, the elements of the reduced state vector reflect the weight or importance of each spatial basis function or principal vector at each time step. Some of these principal vectors are insignificant for all times and can be excluded from the problem entirely, achieving further model reduction. The "importance" of each principal vector depends on the relative amount of variability the corresponding principal component captures within the snapshot dataset. From PCA, the relative variance of each principal component is equivalent to the eigenvalue associated with its principal vector (eigenvector). Therefore, one can control the degree of accuracy by keeping only those eigenvalues whose sum encompasses a desired amount of the variability within the snapshot dataset.

In summary, the determination of the matrix $\mathbf{P}$ and hence the subspace onto which the

model is to be projected is as follows.

1. Perform a full-model run for each well with a constant unit flow rate. At the appropriate time steps record the solution (*i.e.*, drawdown distribution). These solutions are the snapshots. Note that each run should only have one active well.

2. Normalize and group all the snapshots into the matrix, $\mathbf{X}$. Conduct a spectral decomposition of $\mathbf{C}_s = \mathbf{X}^T\mathbf{X}$ and use Equation (2.6) to obtain the matrix of principal vectors.

3. Omit any insignificant principal vectors to from the basis, $\mathbf{P}$.

2.2.2 Galerkin Projection

Once the projection matrix, $\mathbf{P}$, has been determined, the full model must be projected onto the subspace V. Let $L(\mathbf{s}) \in \mathbb{R}^n$ be the residual from Equation (2.3):

$$L(\mathbf{s}) = \mathbf{B}\frac{\partial \mathbf{s}}{\partial t} + \mathbf{A}\mathbf{s} - \mathbf{q} \tag{2.7}$$

The problem of finding the solution of the full model (*i.e.*, solving $L(\mathbf{s}) = 0$) can be equivalently written as finding the vector $\mathbf{s} \in \mathbb{R}^n$ such that $L(\mathbf{s})^T\mathbf{z} = 0, \forall \mathbf{z} \in \mathbb{R}^n$. The Galerkin projection step of POD is now easily defined as

$$\begin{gathered} \textit{find the vector } \hat{\mathbf{s}} \textit{ such that :} \\ L(\hat{\mathbf{s}})^T\mathbf{v} = 0, \forall \mathbf{v} \in V \end{gathered} \tag{2.8}$$

Since any vector, $\mathbf{v} \in V$, can be written as some linear combination of the vectors in the basis, $\mathbf{P}$, the Galerkin projection is simply: $\mathbf{P}^T L(\hat{\mathbf{s}}) = \mathbf{0}$. Applying this projection to Equation (2.3) results in the following,

$$\mathbf{P}^T\mathbf{B}\frac{\partial \hat{\mathbf{s}}}{\partial t} + \mathbf{P}^T\mathbf{A}\hat{\mathbf{s}} = \mathbf{P}^T\mathbf{q} \tag{2.9}$$

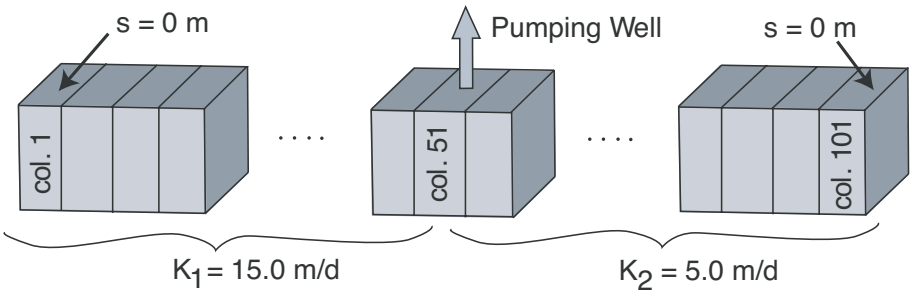

Figure 2.1: One-dimensional groundwater flow model.

Substituting the interpolation shown in Equation (2.4), Equation (2.9) becomes a system of n_p, linearly independent, ODEs and n_p unknowns (assuming the natural system dynamics have been removed):

$$\mathbf{P}^T\mathbf{B}\mathbf{P}\frac{d\mathbf{s}_r}{dt} + \mathbf{P}^T\mathbf{A}\mathbf{P}\mathbf{s}_r = \mathbf{P}^T\mathbf{q} \tag{2.10}$$

Letting, $\tilde{\mathbf{B}} = \mathbf{P}^T\mathbf{B}\mathbf{P}$, $\tilde{\mathbf{A}} = \mathbf{P}^T\mathbf{A}\mathbf{P}$ and $\tilde{\mathbf{q}} = \mathbf{P}^T\mathbf{q}$, we obtain

$$\tilde{\mathbf{B}}\frac{\partial\mathbf{s}_r}{\partial t} + \tilde{\mathbf{A}}\mathbf{s}_r = \tilde{\mathbf{q}} \tag{2.11}$$

This reduced system of ODEs can be solved by any stable time stepping technique, such as Implicit Euler or Crank-Nicolson methods. However, because of its drastically reduced size ($n_p \ll n$), often by several orders of magnitude, the system can also be solved very efficiently by analytical methods via matrix exponential.

2.2.3 One-Dimensional Test Case

A synthetic experimental setup, illustrated in Figure 2.1, from *McPhee and Yeh* [25] was used to exemplify the use of POD. The specific storage is 1.0 m^{-1} and the width of each column is 1.0 m. There are Dirichlet boundary conditions at columns 1 and 101. This test case and all other experiments in this study were modeled by separating the natural system dynamics from the drawdown due to pumping using the superposition principle [3]. Model

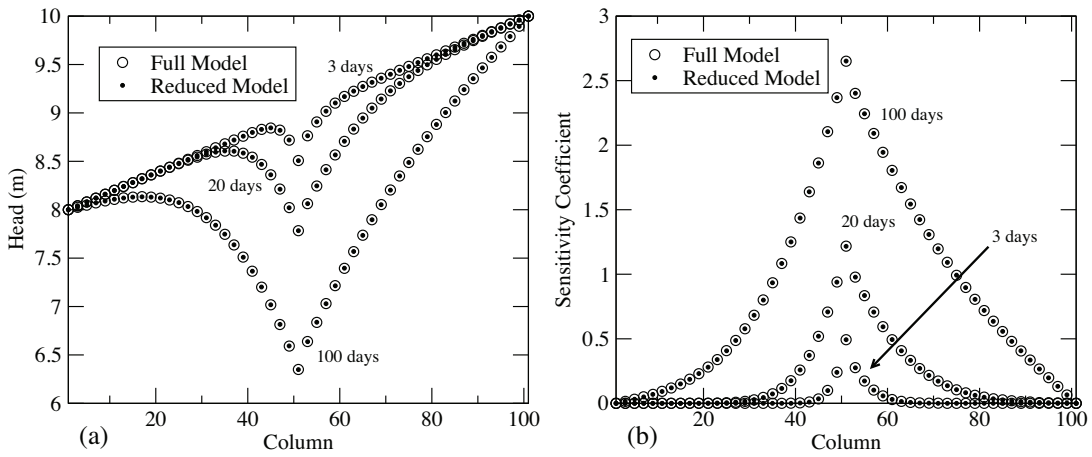

Figure 2.2: (a) Drawdown results of both the full and reduced models after 3, 20 and 100 days for the one-dimensional test case. (b) Sensitivity coefficient results of both the full and reduced models after 3, 20 and 100 days for the one-dimensional test case.

reduction is applied to the groundwater model of drawdown. Therefore, the initial conditions are 0 m everywhere and the Dirichlet boundary conditions at columns 1 and 101 are 0 m. The extraction rate applied to column 51 is 1 m^3/d. The reduced model was developed using 10 snapshots taken at 0.6, 1.5, 2.9, 5.1, 8.5, 13.9, 22.4, 35.6, 56.4 and 89.1 days (n_s = 10). Figure 2.2a displays the drawdown results of both the full and reduced models of the one-dimensional test case. The results of the reduced model are indistinguishable with that of the full model. Note that the Dirichlet boundary conditions are met naturally when drawdown is used as the dependent variable. *McPhee and Yeh* [25] applied POD model reduction to head and reported difficulty in satisfying the boundary conditions.

The sensitivities of the heads with respect to pumping (*i.e.*, the impact changes in pumping will have on drawdown) were also calculated using a simple finite difference approach. Figure 2.2b illustrates these sensitivities for both the full and reduced models. Again, the results of the reduced model are indistinguishable with those of the full model. Note that the time steps for which the results have been displayed do not coincide with those of the snapshots used to develop the reduced model. In this example, the full model consists of 101 equations and the reduced model consists of 10 equations, creating a reduction in model

dimension of one order of magnitude.

2.3 Snapshot Selection

The ability of a reduced model, obtained from POD, to accurately represent and, in practice, replace the full model is based solely on the manner in which the full model snapshots are obtained. Both the number of snapshots, as well as the time steps in which they are taken, affect the accuracy of the reduced solution. However, a large number of snapshots will not necessarily result in a high level of accuracy. Therefore, the goal is to find the best sampling strategy for a given snapshot size such that the accuracy of the reduced model is maximized.

There are many ways to approach this problem. In this paper we define the "best" sampling times for snapshots by requiring that all snapshots be significant in the amount of information that they possess. In other words, after conducting PCA, the number of normalized eigenvalues significantly different from zero should be maximized in order to maintain the desired level of accuracy within the reduced model (provided the snapshot size, n_s, is large enough). The number of snapshots is optimal when the addition of another snapshot does not add a significant amount of information to the reduced model. For example, the addition of one snapshot which, after PCA, results in the same number of significant principal vectors as before the snapshot was added is indicative that increasing the snapshot size (*i.e.*, the number of snapshots) was unnecessary. This can be thought of as adding a snapshot which is approximately a linear combination of the other snapshots; thus, providing little additional information. Of course, when the snapshot size is increased, the optimal times in which all of the snapshots are taken must be reevaluated.

2.3.1 Exponentially Distributed Snapshots

In order to determine the best snapshot times, for any POD model reduction, the dynamic properties of the governing equation must be taken into consideration. In the case of saturated groundwater flow, the governing equation is a parabolic PDE, indicating the system is diffusive in nature. These types of transient models tend to exhibit rapid changes in the state variable for early times and small changes for later times. In other words, these types of systems reach steady state at an exponential rate [19]. Therefore, to fully capture the dynamics of the system, one must acquire many snapshots early in time and fewer snapshots later in time. For example, if many snapshots were taken near steady state, they would be approximately equal and the corresponding covariances would be small, resulting in small eigenvalues and insignificant principal vectors. If few snapshots were taken at early time steps where the shape of the state variable distribution is changing rapidly, interpolations between these snapshots (*i.e.*, the reduced model) could be inaccurate.

To study these properties we look at the analytical solution of Equation (2.3), which can be written as

$$\mathbf{s}(t) = e^{-\mathbf{B}^{-1}\mathbf{A}t}\left[\mathbf{s}_0 - \mathbf{A}^{-1}\mathbf{q}\right] + \mathbf{A}^{-1}\mathbf{q} \tag{2.12}$$

The above matrix exponential can be evaluated by means of the solution to the generalized eigenproblem $\mathbf{Au} = \lambda\mathbf{Bu}$, where matrices $\mathbf{A}$ and $\mathbf{B}$ are symmetric and positive definite. The drawdown vector is then given as

$$\mathbf{s}(t) = \mathbf{U}e^{-\mathbf{M}t}\mathbf{U}^T\left[\mathbf{s}_0 - \mathbf{A}^{-1}\mathbf{q}\right] + \mathbf{A}^{-1}\mathbf{q} \tag{2.13}$$

where matrix $\mathbf{U}$ is the unitary matrix of the generalized eigenvectors and $\mathbf{M}$ is a diagonal matrix containing the generalized eigenvalues $\mu_i > 0$. Thus it is clear that only the smaller eigenvalues and corresponding eigenvectors are necessary to capture the transient behavior

of the solution. The question is then how can we select the times of the snapshots so that the information contained in this set of vectors is maximized. The approach proposed in this research is illustrated by working on a simple scalar ODE, whose solution can be directly written as

$$y(t) = ce^{-\alpha t} + b \tag{2.14}$$

Introducing the scaled time $t^* = e^{-\alpha t}$ the behavior of $y(t^*)$ becomes linear. Thus, the interval of the scaled time can be subdivided uniformly without loss of accuracy. Hence the times of the snapshots are defined with the following function:

$$t_s = \beta e^{-\alpha t_u} + \gamma \tag{2.15}$$

where α, β and γ are parameters to be determined on the basis of the equation properties (*i.e.*, hydraulic conductivity, elastic storage, etc.), while t_u varies uniformly within an appropriate interval of length T such that $t_u = uh$, $u = 0, \ldots, n_s - 1$ where $h = T/(n_s - 1)$. For example, we can choose $T = 10$ and $n_s = 5$ such that $t_u = 0$, 2.5, 5, 7.5, 10. We observe that the snapshot time coincides with $\beta + \gamma$ for $u = 0$, and with γ for large t_u, *i.e.*, "pseudo" steady state conditions. Thus, given a fixed number of snapshots and values for α, β and γ, we can determine a snapshot set with an exponential distribution in time.

We define the solution error of the reduced model at a particular time step t_k as the Euclidian norm of the error between the reduced-model and the full-model solutions:

$$\tau_r(t_k) = \sqrt{\sum_{i=1}^{n} \left(\mathbf{p}_i^T \mathbf{s}_r(t_k) - \mathbf{s}_i(t_k)\right)^2} \tag{2.16}$$

where $\mathbf{p}_i$ is a vector consisting of the i-th row of the basis $\mathbf{P}$. Using our snapshot selection strategy, the solution error will depend only on the number n_s of snapshots and the values

of the parameters α, β and γ. Thus the "optimal" reduced model can be identified by the following minimization problem:

$$\min_{n_s,\alpha,\beta,\gamma} \left[\text{ARMSE} = \frac{1}{T} \int_0^T \tau_r(t) dt \right] \tag{2.17}$$

where ARMSE is the Average Root Mean Square Error and T is the ending time of the simulation. The time integral in the formula is evaluated for ARMSE by means of a 3-point Gaussian quadrature rule. Given that $\tau_r(t_k)$ varies smoothly with time, this Gaussian quadrature rule is sufficiently accurate to ensure that its error is always smaller than the error being evaluated. It is obvious that the optimal n_s, α, β and γ depend upon the hydrological parameters, among other factors, and must be determined case by case. Extending these results to the general case, we need to relax absolute optimality and look for a "suboptimal" but still accurate reduced-model solution. To accomplish this, we apply our selection procedure to a dimensionless model and translate this result to any real model using an approximation or averaging technique to account for heterogeneities and complex geometries within the real model. This technique is described in subsequent sections.

2.3.2 Optimal Snapshot Set - Dimensionless Model

Equation (2.15) was applied to the one-dimensional test case in Figure 2.1. The preliminary results of this experiment indicated that the best snapshot sets would include the very first time step of the numerical model, *i.e.*, a snapshot at a very early time. This makes sense since having a snapshot as close to the initial condition as possible will accurately capture the behavior of the system at early times. One may reasonably assume that the optimal snapshot set would always include the drawdown distribution at early times and the drawdown distribution representative of steady state conditions. Therefore, an effective

exponential snapshot selection method will be one in which the initial and final snapshot times are fixed accordingly. For a given value of γ, there is one value for α and one value for β such that the initial and final snapshot times produced by equation (2.15) agree with the corresponding desired values. Therefore, the optimal exponential snapshot set is found by determining the optimal value for the parameter γ.

Even though this method will result in an accurate reduced model, determining the optimal γ value for a large-scale model can be computationally demanding. One would have to use a fine temporal discretization and record the solution for the entire model domain at every time step, then construct the reduced model for every value of γ and compute an error criterion that would be used to determine the optimal value for γ. This process would have to be repeated for every well. However, if one were to use this process for the dimensionless model and could then translate the result to any real-world model, the computational requirement would be greatly reduced. Note that this translation can only be approximated at best. Since the optimal snapshot set varies with the parameters of the system (hydraulic conductivity, specific storage, etc.) and the physical geometry of the system, in principle we cannot exactly translate the optimal snapshot set developed from a dimensionless model to that of a heterogeneous model with a non-regular domain.

We address this problem as follows. Define the dimensionless time as [3]

$$\bar{t}_s = \frac{K}{S_s L^2} t_s = C t_s \tag{2.18}$$

where $\bar{t}_s$ is the snapshot time of the dimensionless model and L, K, and S_s are the characteristic length, hydraulic conductivity, and specific storage of the real-world system, respectively. This equation is exact only if the real-world model is homogeneous and has the same shape as the dimensionless model. Using representative values for the parameters and system size (*e.g.*, average hydraulic conductivity, etc.), the optimal snapshot selection determined for

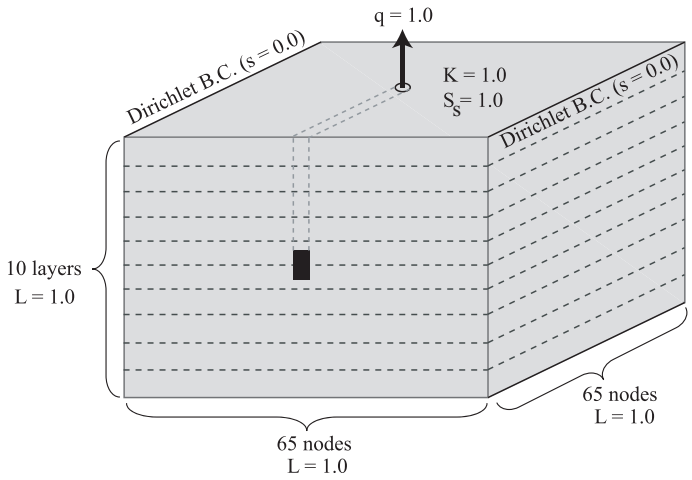

Figure 2.3: Experimental setup for the threedimensional dimensionless model.

the dimensionless model can be translated, approximately, to any real-world model using equation (2.18). However, instead of looking for representative values of the parameters, we can proceed by noting that the ratio between the dimensionless times and real-world time is a constant, $\bar{t}_s/t_s = C$, encompassing the representative values of the parameters and the geometry. Hence, we can evaluate this constant by looking at the pseudo-steady state times for the dimensionless and the real-world model, and then all the snapshot times can be translated using this constant. Of course, the resulting real-world snapshot set would only be approximately optimal; however, we expect that slight deviations in snapshot times from the optimal set would yield insignificant changes in the reduced-model accuracy.

This methodology was applied to the dimensionless, confined, homogeneous, isotropic, aquifer in three dimensions (Figure 2.3). SAT3D, a linear threedimensional finite element, saturated groundwater flow model was used to calculate drawdown given forcing [16]. All parameters and spatial dimensions were set equal to 1.0 in the dimensionless model, which has been uniformly discretized with a nodal arrangement of $65 \times 65 \times 11$ resulting in 46,475 nodes and 245,760 tetrahedral elements. Zero Dirichlet boundary conditions are applied across two faces of the cube opposite one another. The initial conditions are $s = 0$ everywhere. To determine the time of pseudo-steady state, the observation network depicted in Figure 2.4

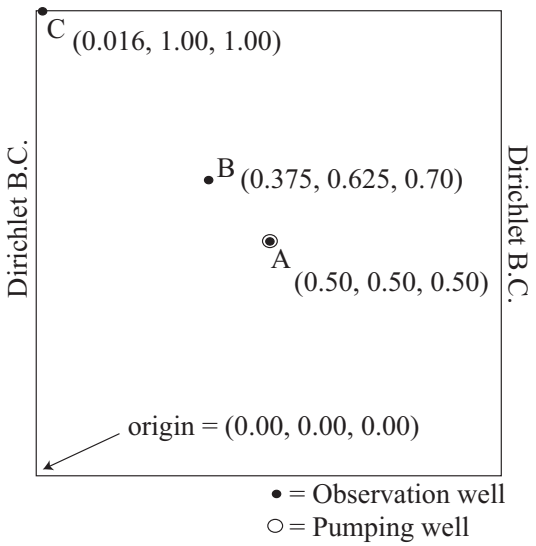

Figure 2.4: Locations of observation and pumping wells for the dimensionless model.

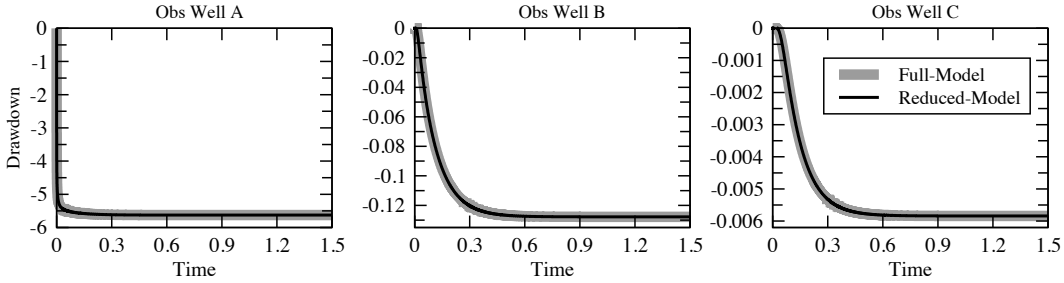

Figure 2.5: Time behavior of the drawdown of the dimensionless model at well locations shown in Figure 2.4.

was used. The results of a single forward simulation are shown in Figure 2.5. Accordingly, the system reaches steady state quite rapidly near the pumping well, so rapidly that the initial snapshot must be taken at $t_1 = 1.0 \times 10^{-7}$. At this initial time step the drawdown is on the order of 5.0×10^{-3} at the location of the well, whereas at steady state, the drawdown is on the order of 5.0. Based on Figure 2.5, the system is clearly at approximate steady state conditions when $t = 0.90$. Therefore, the initial and final snapshots will be taken at these times.

Equation (2.15) can be used to generate snapshot sets for various values of γ. Figure 2.6 displays the behavior of the snapshot times for different values of γ. We see that the smaller

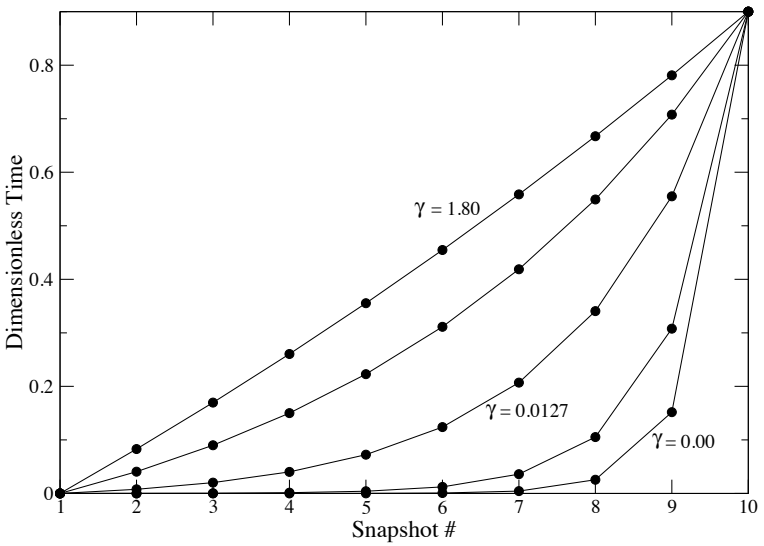

Figure 2.6: Behavior of snapshot times for different values of the parameter γ in Equation (2.15).

the value of γ, the heavier the emphasis on early time steps. When $\gamma \approx 1.80$, the snapshot selection is approximately linear between the initial and final snapshot times. Obtaining the optimal snapshot set when using a numerical model presents some practical difficulties. For example, the numerical model solves the system at discrete time steps, whereas the exponential snapshot distribution, described by Equation (2.15), is continuous. Therefore, the results of the continuous snapshot selection must be rounded to the corresponding nearest model time steps. In addition, capturing snapshots at very early time steps requires variable time stepping in the numerical model. For this exercise, the time stepping is variable and consists of 2,075 time steps to ensure accuracy in the calculations. In practice, coarser time steps can actually be used. We chose to work with $n_s = 10$ snapshots. The initial snapshot is fixed at $t_1 = 1.0 \times 10^{-7}$ and the final snapshot is always $t_{10} = 0.90$. However, in between, the snapshot times are rounded to the nearest model time step.

Optimality Criterion

The criterion needed to define optimality for the values of n_s and γ must now be determined. As mentioned before, in principle, we would like to find the snapshot set that minimizes the

solution error, *i.e.*, solves problem (2.17). However, the relationship between γ and ARMSE is complicated, being strongly affected in particular by the PCA step of the POD algorithm. Therefore, instead of using ARMSE as a criterion, one could employ experimental design criteria in which the goal is to maximize the information contained in the snapshot covariance matrix. The approach would be similar to using the E-optimality criterion where, in the context of experimental design, the objective is to minimize the maximum eigenvalue of the parametric covariance matrix [45]. We may think of the best snapshot set as being the one that yields PCA principal components that are all significant in terms of variance accounted for, *i.e.*, for which all the values of ϕ_j of equation (2.5) are significant. Hence, our objective is to maximize the minimum eigenvalue $\lambda_{\min}$ of the state covariance matrix $\mathbf{C}$ generated from the snapshots. The latter is the criterion of choice.

Numerical Results

This criterion is pplied to the dimensionless model described above. The best value for γ is numerically obtained via exhaustive search. Snapshot sets of 10 snapshots each are generated for 40 values of γ and the corresponding minimum eigenvalues are calculated. The results are displayed in Figure 2.7, where the behavior of $\lambda_{\min}$ versus γ is shown. The curve displays a distinct maximum when $\gamma = 3.87 \times 10^{-6}$, which is thus the optimal value. Some oscillations and negative eigenvalues begin to appear when γ is large, due to numerical errors for very small eigenvalues, a sign that the covariance matrix becomes ill-conditioned.

In addition to determining optimal snapshot times, one must also address the size of the snapshot set, *i.e.*, how large must the snapshot set be such that the reduced model is sufficiently accurate. To explore this problem, we develop optimal snapshot sets, using the aforementioned method and dimensionless model, for sizes of 4, 7 and 10 snapshots. To compare each snapshot size, we need to ascertain the solution accuracy (ARMSE defined in Equation (2.16)) with respect to the full model. Although, the ARMSE is not a good

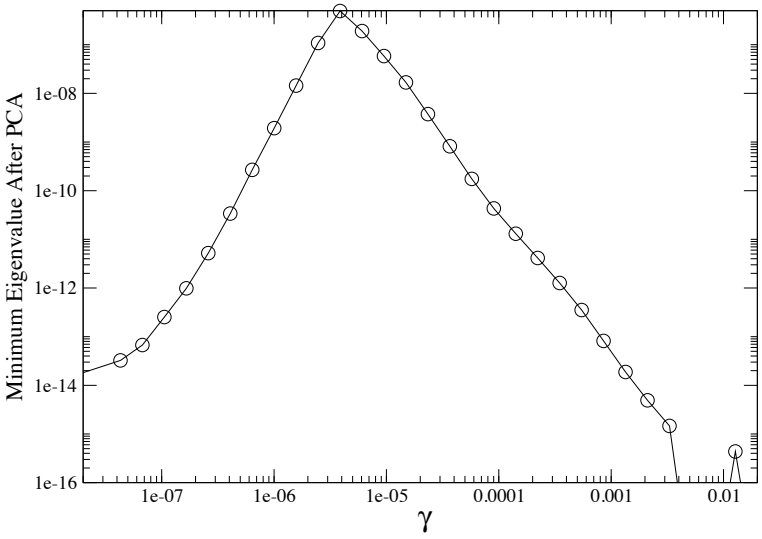

Figure 2.7: Relationship between γ and the minimum eigenvalue of the covariance matrix after PCA.

criterion for snapshot determination, it can still be used to gauge model agreement. The ARMSE values were 3.09×10^{-3}, 2.74×10^{-5}, and 3.36×10^{-6} for snapshot sizes of 4, 7 and 10, respectively. Clearly, a snapshot size of 10 will produce a sufficiently accurate reduced model. Figure 2.5 shows both the full and reduced-model results for 3 nodes at all time steps using 10 snapshots and Table 2.1 lists the optimal snapshot times. Based on these results, the 10-snapshot reduced model is in excellent agreement with the full model. Note that the full-model system of 46,475 ODEs (n) has been reduced to a system of 10 ODEs (n_s) for a single well, creating a reduction in model dimension of more than three orders of magnitude. This can be reduced even further by omitting insignificant principal vectors from the basis, $\mathbf{P}$; n_p is usually equal to 3 for a single well.

2.3.3 Dimensionless Versus Heterogeneous Models

In this section, we verify the proposed method of translating the snapshot times of the dimensionless model to a real-world model. The real-world model is represented by a "realistic" synthetic model with dimensions $5,000$ m $\times$ $3,000$ m $\times$ 100 m. The discretization

Table 2.1: Optimal snapshot sets for the dimensionless and realistic models along with approximate optimal snapshots for the realistic model determined from translating dimensionless times into realistic times.

Snapshot Number	Optimal Snapshot Set		Approximate Optimal Snapshot Set for Realistic Model (d)
	Dimensionless	Realistic (d)	
1	1.00E-07	1.42E-04	1.42E-04
2	1.18E-05	8.06E-03	1.67E-02
3	5.76E-05	4.24E-02	8.18E-02
4	2.38E-04	1.91E-01	3.38E-01
5	9.49E-04	8.35E-01	1.35E+00
6	3.75E-03	3.62E+00	5.32E+00
7	1.48E-02	1.57E+01	2.10E+01
8	5.81E-02	6.81E+01	8.25E+01
9	2.29E-01	2.95E+02	3.25E+02
10	9.00E-01	1.28E+03	1.28E+03

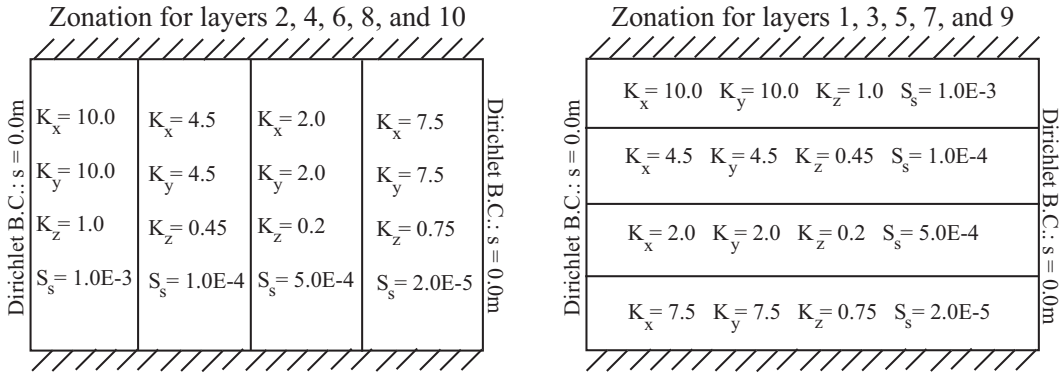

Figure 2.8: This diagram displays, in plan view, the zonation pattern and parameter values used in the realistic model.

for this model is the same as that of the dimensionless model: 46,475 nodes and 245,760 tetrahedral elements. The model contains 10, uniformly spaced, layers and each layer has 4 zones. Figure 2.8 shows the zonation of each layer. A well is placed in the center of the model domain with a constant extraction rate. The initial conditions are zero drawdown throughout the model domain.

Upon running the simulation and observing the drawdowns at various locations within the model domain, we conclude that the system reaches pseudo-steady state conditions after approximately 3.5 years (1,278 days). The optimal snapshot set ($n_s = 10$) was rigorously determined for this realistic model by maximizing $\lambda_{\min}$; the optimal snapshot times are listed

in Table 2.1. Using the pseudo-steady state times of both the realistic and dimensionless models, the constant, C (equation (2.18)), can be determined, and the optimal snapshots of the dimensionless model can be translated to approximate those of the realistic model. These approximated snapshots are listed in Table 2.1. The snapshot set from the approximation is very similar to that determined by numerically maximizing $\lambda_{\min}$. The ARMSE for the approximation and the formally optimized snapshots sets, with respect to the full model, are 3.68×10^{-4} m and 5.52×10^{-4} m, respectively. Note that the ARMSE for the approximation is slightly smaller than that determined from maximizing $\lambda_{\min}$. However, the ARMSE for both cases is very small suggesting that the proposed translation of snapshot times from the dimensionless model to any real-world model will likely yield a reduced model just as accurate as if one were to conduct a formal optimization of snapshot times for the real-world model itself. For this exercise, determining the optimal snapshot set for the realistic model by maximizing $\lambda_{\min}$ required 14 hours of CPU time using an Intel Pentium 4, 3.0 GHz, processor with a 512 KB L2 cache; whereas, the proposed translation method requires less than a second because the optimal snapshot times of the dimensionless model are predetermined.

2.4 Application: Central Veneto, Italy

The applicability of the proposed methodology is demonstrated on a large aquifer model developed for management purposes. The aquifer is located in Northeast Italy and serves a population of a few million people in addition to agricultural and industrial demands.

2.4.1 Site Description

The Upper and Central Veneto Plain in Northern Italy (Figure 2.9, top) is characterized by abundant subsurface water resources that are heavily exploited for industrial, agricultural, and civil uses, serving a population of about 3 million people. The area of interest is situated

in the piedmont plain and is delimited on the west from the Lessini mountains and the Berici hills, on the north from Asiago plateau, on the east from the Brenta river and on the south from the Adriatic Sea. The aquifer system is characterized to the north-west by an undifferentiated unconfined formation recharged directly by copious precipitation collected by the Asiago Plateau. The area is characterized by the presence of spatially distributed groundwater springs localized in an area overlying the transition zone from an unconfined aquifer (in the north of the area) to confined aquifers (in the south) (Figure 2.9, top). The multiaquifer system originating in this area is formed by five highly productive aquifers that are the main source for potable water in the surrounding region. These aquifers extend aerially towards the southeast until they are pinched out by the Santerno Formation, a thick clay layer that confines from below the Quaternary deposits and surfaces on the eastern boundary of the Adriatic Sea. The well-developed basement of the Central Veneto aquifer system surfaces on the northern boundary and reaches about 500 m in depth on the southern boundary [29].

In recent years, water extraction has exceeded recharge and as a result, most of the observation wells in the area show a trend of decreasing head levels. For this reason, public authorities have commissioned the development of a fully 3-dimensional groundwater flow model to help in the determination of management strategies. The model, described in detail by *Passadore et al.* [29], uses a finite element method based on linear tetrahedral elements defined on a mesh of 143,496 nodes and 831,790 tetrahedral elements. The version of the model used in this study was refined to 222,687 nodes and 1,289,570 tetrahedral elements. The highly unstructured mesh and the large number of elements were dictated by the need to accurately capture the behavior of the unconfined-confined transition zone. This requires an accurate geometrical description of the pinch-outs in the low permeability lenses. Calibration was performed by minimizing the squared difference between simulation results and observation data collected at more than 100 wells in the area. The unconfined

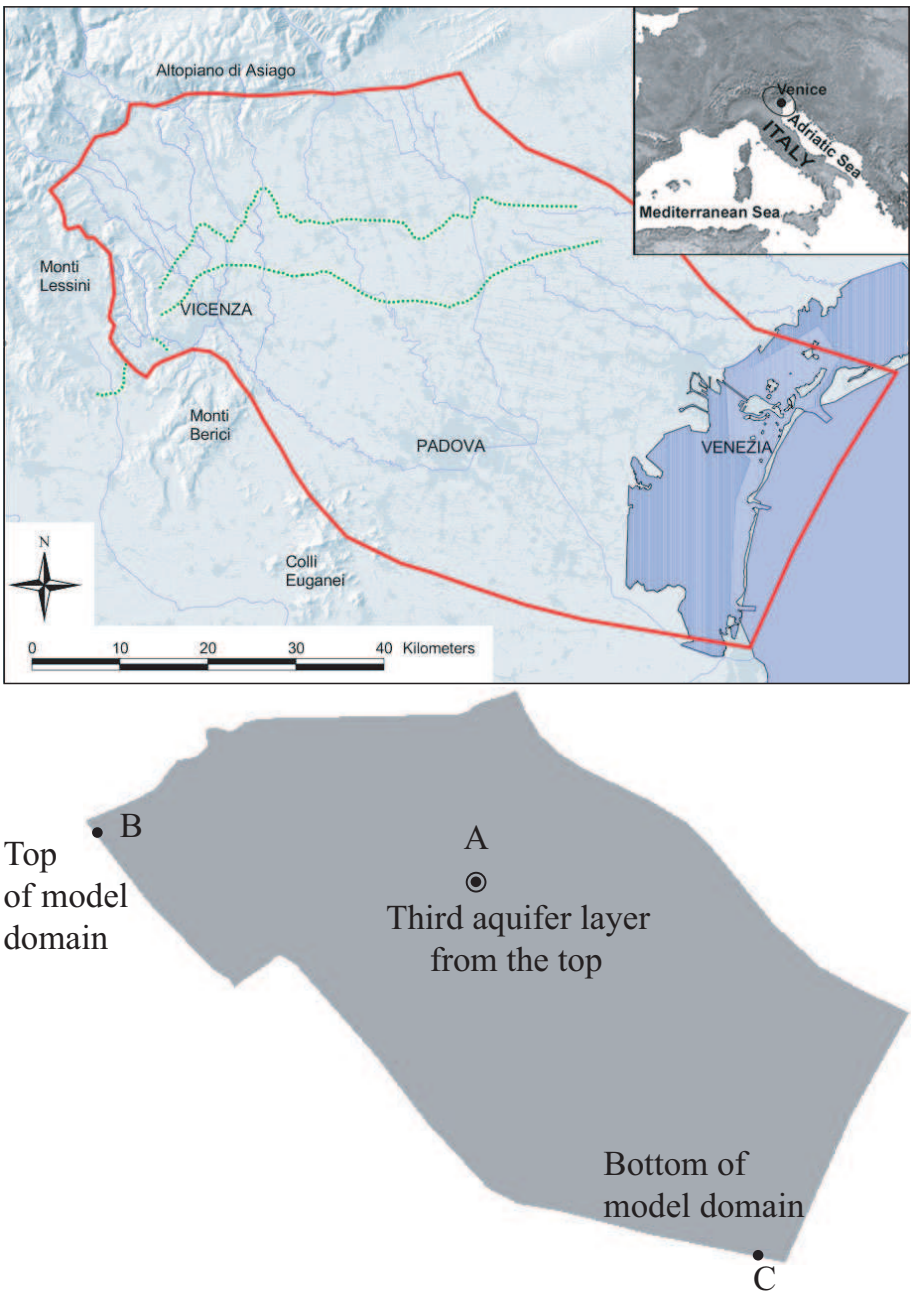

Figure 2.9: (top) Planar view of the Central Veneto model domain. (bottom) Locations of the pumping and observation wells for model reduction of the Central Veneto model.

Table 2.2: Optimal Snapshot Set for the Dimensionless Model and Approximate Optimal Snapshot Set for the Central Veneto Model.

Snapshot Number	Optimal Snapshot Set for Dimensionless Model	Approximate Optimal Snapshot Set for Central Veneto Model (yrs)
1	1.00E-07	4.40E-07
2	1.18E-05	5.18E-05
3	5.76E-05	2.54E-04
4	2.38E-04	1.05E-03
5	9.49E-04	4.18E-03
6	3.75E-03	1.65E-02
7	1.48E-02	6.50E-02
8	5.81E-02	2.56E-01
9	2.29E-01	1.01E+00
10	9.00E-01	3.96E+00

aquifer was subdivided into 50 material zones to capture the highly heterogeneous structure of a geological formation complicated by the presence of several paleoriverbeds.

2.4.2 Application of POD

To demonstrate the application of the aforementioned snapshot selection method, we consider a single well located near the center of the model domain (Figure 2.9). The timing of approximate steady state conditions is calculated using several observation wells located throughout the model domain. After some experimentation, location C in Figure 2.9 was determined to be an appropriate indicator as to when approximate steady state conditions are reached for the entire model domain (*i.e.*, drawdown at this location will take the longest time to reach pseudo-steady state). After visual inspection of the drawdown curves in Figure 2.10, approximate steady conditions, similar to those in the dimensionless case, occur four years after constant pumping has begun. Table 2.2 lists the optimal snapshot times of the dimensionless model and those corresponding to the Central Veneto model.

The first time step of the Central Veneto numerical model was set to 4.4×10^{-7} years (13.9 sec) and the length of each time step is multiplied by a factor of 1.03 until this length

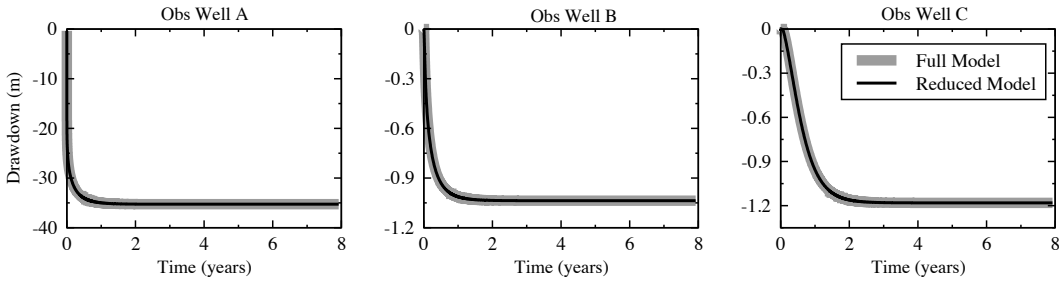

Figure 2.10: Time behavior of the calculated drawdowns at the well locations shown in Figure 9 for the Central Veneto Models.

Table 2.3: RMSE Values, Over the Entire Model Domain, for Comparison Between the Full and Reduced Central Veneto Models.

Time(yrs)	RMSE (m)
3.20E-04	2.15E-03
3.20E-02	2.02E-02
1.60E-01	1.82E-02
3.20E-01	8.31E-03
4.80E-01	1.18E-02
6.30E-01	7.80E-02
9.50E-01	1.08E-03
1.30E+00	1.47E-03
1.90E+00	8.41E-04
3.20E+00	5.56E-05

reaches 1 day, after which the time step is fixed at 1 day. The snapshots were then acquired as closely to the times listed in Table 2.2 as possible. The CPU time required to solve the system of equations at all time steps using a workstation with an Intel Pentium 4, 3.0 GHz, processor with a 512 KB L2 cache was 15.3 hours. Using the snapshots acquired from this simulation, the reduced model required only 56 seconds to run the same simulation on the same machine. This is a reduction in CPU time of 1000 times. Note that the full-model system of 222,687 ODEs (n) has been reduced to 10 ODEs (n_s) with a single well, which can be reduced even further to n_p ODEs by omitting insignificant principal vectors from the basis, $\mathbf{P}$. The results of both simulations are displayed in Figure 2.10 for the locations depicted in Figure 2.9. The RMSE was also calculated for the entire domain at 10 time steps and listed in Table 2.3.

The slightly larger ARMSE values in the early time steps are a result of some oscillations,

on the order of a few millimeters, at locations far from the pumping well where the drawdown is essentially 0 m. This phenomenon is also apparent in the dimensionless case as well. However, these oscillations are so small as to be insignificant in practice. The reduced model is an extremely accurate surrogate model that runs 1000 times faster than the full model. Therefore, the reduced model now allows one to analyze scenarios that require several hundreds or even thousands of model runs such as, optimization, data assimilation, Monte Carlo uncertainty analysis, etc.

Chapter 3

Reduced Order Parameter Estimation using Quasilinearization and Quadratic Programming

3.1 Confined aquifer groundwater flow model

The following PDE describes two-dimensional groundwater flow for a confined, anisotropic aquifer with pumping [3]:

$$\frac{\partial}{\partial x}\left(bK_x\frac{\partial h}{\partial x}\right)+\frac{\partial}{\partial y}\left(bK_y\frac{\partial h}{\partial y}\right)-q-bS_s\frac{\partial h}{\partial t}=0, \tag{3.1}$$

with initial and boundary conditions:

$$
\begin{aligned}
h(x,y,0) &= h_0(x,y); \\
h(x,y,t) &= h_d(x,y,t),\ (x,y,t) \in (\Gamma_1); \\
\left(bK_x \frac{\partial h}{\partial x} n_x + bK_y \frac{\partial h}{\partial y} n_y \right)(x,y,t) &= q_n(x,y,z,t),\ (x,y,t) \in (\Gamma_2),
\end{aligned}
\tag{3.2}
$$

where h is the hydraulic head (L); $K_x(x,y)$, $K_y(x,y)$ are spatially varying hydraulic conductivities in the x and y directions, respectively (L/T); S_s is the specific storage (L^{-1}); $b(x,y)$ is the thickness of the aquifer (L); q is the specific volumetric pumping rate (LT^{-1}); Γ_2 is the flux boundary; Γ_1 is the fixed head boundary; and h_0 , h_d , and q_n are known functions. For simplicity and without loss of generality, we assume isotropic behavior of the aquifer, *i.e.*, $K_x = K_y = k(x,y)$.

The application of the superposition principle to Equation (3.1) followed by spatial discretization of the resulting PDE (*e.g.*, by finite differences, finite elements, etc.) yields a system of linear ordinary differential equations (ODEs) for the drawdown, $\mathbf{s}$:

$$
\mathbf{B}\frac{d\mathbf{s}}{dt} = \mathbf{A}\mathbf{s} + \mathbf{q} = \mathbf{f}(\mathbf{s},\mathbf{k}),
\tag{3.3}
$$

where $\mathbf{A}$ is the $n \times n$ stiffness matrix; $\mathbf{B}$ is the $n \times n$ mass matrix; $\mathbf{s}$ and $\mathbf{q}$ are the $n-$dimensional vectors of nodal (cell) drawdowns and source/sinks, respectively; $\mathbf{f}(\mathbf{s},\mathbf{k}) = \mathbf{A}\mathbf{s} + \mathbf{q}$ is a vector-valued function depending on drawdown $\mathbf{s}$ and hydraulic conductivity $\mathbf{k}$; and n is the number – generally very large – of spatial computational nodes (cells). The n_z-dimensional vector $\mathbf{k}$ represents the spatially varying hydraulic conductivity, which is assumed to be discretized into n_z material zones. In the majority of cases of practical interest, matrices $\mathbf{A}$ and $\mathbf{B}$ are large, sparse, symmetric and positive definite. Upon the application of an Implicit Euler scheme, Equation (3.3) can be approximated as

$$
\left(\mathbf{A} - \frac{1}{\Delta t_j}\mathbf{B} \right) \mathbf{s}_j = -\frac{1}{\Delta t_j}\mathbf{B}\mathbf{s}_{j-1} - \mathbf{q}_j,
\tag{3.4}
$$

where $\mathbf{s}_j$ and $\mathbf{q}_j$ are vectors of nodal drawdown and extraction rate values at time j, respectively; and Δt_j is the length of the j-th time step.

3.2 Groundwater parameter estimation via quasilinearization and quadratic programming

3.2.1 Problem Formulation

The primary goal of parameter estimation is to identify the parameter vector that minimizes some norm of the residuals, *i.e.*, differences between the model-predicted state variable(s) and those observed in the field. The most commonly used objective for this class of problems is minimizing the sum of the squared residuals. The parameter vector of interest for this study consists of the zonal hydraulic conductivity values, $\mathbf{k}$. The state vector of interest consists of the nodal (cell) drawdown values, $\mathbf{s}$. Note that generally, matrix $\mathbf{A}$ in Equations (3.3) and (3.4) is the only term that explicitly contains the vector $\mathbf{k}$. Therefore, the general problem statement can be written as

$$\begin{aligned} &\min_{\mathbf{k}} \sum_{j=1}^{n_t} \sum_{i=1}^{n_j} \left(s_{\mathscr{K}_j(i)} - s^*_{i,j} \right)^2 \\ &\text{subject to:} \\ &\left(\mathbf{A} - \frac{1}{\Delta t_j} \mathbf{B} \right) \mathbf{s}_j = -\frac{1}{\Delta t_j} \mathbf{B} \mathbf{s}_{j-1} - \mathbf{q}_j, \quad j = 1, \ldots, n_t \\ &\mathbf{k}_{\min} \leq \mathbf{k} \leq \mathbf{k}_{\max} \end{aligned} \tag{3.5}$$

where n_t is the number of time steps; n_j is the number of observation locations at time step j; $s_{\mathscr{K}_j(i),j}$ and $s^*_{i,j}$ are the drawdown values, for measurement location i and time j, predicted by the model and observed in the field, respectively; and $\mathscr{K}_j(i)$ maps the position of the

appropriate computational node (cell) to its corresponding $i-$th observation at time j.

3.2.2 Quasilinearization and Quadratic Programming

The method of quasilinearization and quadratic programming, as it applies to parameter estimation, consists essentially of solving a series of quadratic programming (QP) sub-problems such that the solution to these problems converges to the solution of the original nonlinear inverse problem. *Yeh* [43] provides a methodology in which the governing equation is linearized about the current estimate of the parameter vector and the state vector using a Taylor series expansion. This linearized equation replaces the original governing equation in the least-squares parameter estimation problem resulting in a QP problem. The solution to this QP problem then becomes the current estimate for a new Taylor series expansion resulting in a new QP. This process is repeated in the linearized system until the solution converges to the solution of the original nonlinear least-squares problem. Consider the governing equations after spatial discretization and before temporal discretization, *i.e.*, the system of ordinary differential equations (ODEs) in Equation (3.3). Applying a Taylor series expansion about some current estimate of the drawdown, $\mathbf{s}^m$, and hydraulic conductivity, $\mathbf{k}^m$, retaining up to the first order terms only, results in the following:

$$\begin{aligned}\mathbf{B}\frac{d\mathbf{s}^{m+1}}{dt} = \mathbf{f}(\mathbf{s}^m, \mathbf{k}^m) + \nabla_{\mathbf{s}}\mathbf{f}(\mathbf{s}^m, \mathbf{k}^m)(\mathbf{s}^{m+1} - \mathbf{s}^m) \\ + \nabla_{\mathbf{k}}\mathbf{f}(\mathbf{s}^m, \mathbf{k}^m)(\mathbf{k}^{m+1} - \mathbf{k}^m)\end{aligned} \tag{3.6}$$

where $\mathbf{s}^{m+1}$ is an approximation of the drawdown, given some new parameter vector, $\mathbf{k}^{m+1}$. The Jacobian matrix of $\mathbf{f}$ with respect to $\mathbf{s}$ is

$$\nabla_{\mathbf{s}}\mathbf{f}(\mathbf{s}^m, \mathbf{k}^m) = \mathbf{A}^m \tag{3.7}$$

where $\mathbf{A}^m$ is the $\mathbf{A}$ matrix in Equation (3.3) comprised of the current estimate of hydraulic conductivity, $\mathbf{k}^m$. The Jacobian matrix of $\mathbf{f}$ with respect to $\mathbf{k}$ can be approximated numerically via finite difference as

$$[\nabla_{\mathbf{k}}\mathbf{f}^m]_{i,j} = \frac{df_i^m}{dk_j} \approx \frac{f_i\left(k_i^m + \Delta k_j\right) - f_i\left(k_j^m\right)}{\Delta k_j} = [\mathbf{D}^m]_{i,j}\,, \tag{3.8}$$

where Δk_j is some relatively small increment of hydraulic conductivity for element j of $\mathbf{k}^m$, and $\mathbf{D}^m \approx \nabla_{\mathbf{k}}\mathbf{f}^m$ contains the current estimate of $\mathbf{s}^m$. Substituting these Jacobian matrices into Equation (3.6) results in the following equation:

$$\mathbf{B}\frac{d\mathbf{s}^{m+1}}{dt} = \mathbf{A}^m\mathbf{s}^m + \mathbf{q} + \mathbf{A}^m(\mathbf{s}^{m+1} - \mathbf{s}^m) + \mathbf{D}^m(\mathbf{k}^{m+1} - \mathbf{k}^m), \tag{3.9}$$

This equation can be rewritten such that it has the same form as the governing equation for groundwater flow (Equation (3.3)), with an additional forcing term associated with changes in hydraulic conductivity:

$$\mathbf{B}\frac{d\mathbf{s}^{m+1}}{dt} = \mathbf{A}^m\mathbf{s}^{m+1} + \mathbf{D}^m(\mathbf{k}^{m+1} - \mathbf{k}^m) + \mathbf{q}, \tag{3.10}$$

At the $m-$th iteration, the Implicit Euler scheme can be used to approximate the solution to Equation (3.10) in time as follows:

$$\left(\mathbf{A}^m + \frac{1}{\Delta t_j}\mathbf{B}\right)\mathbf{s}_j^{m+1} = \frac{1}{\Delta t_j}\mathbf{B}\mathbf{s}_{j-1}^{m+1} + \mathbf{D}_j^m(\mathbf{k}^{m+1} - \mathbf{k}^m) + \mathbf{q}, \tag{3.11}$$

Note that $\mathbf{D}^m$ is a function of time because it contains the current estimate $\mathbf{s}^m$, which is a function of time. The QP sub-problem now can be solved using the linearized equations of

the governing ODEs (equations (3.10) and (3.11)), yielding the following algorithm:

ALGORITHM QQP

Given the initial feasible estimates $\mathbf{k}^0$ and $\mathbf{s}^0$:

For $m = 0, 1, \ldots,$ until convergence, do:

find $\mathbf{k}^{m+1}$ such that:

$$\min_{\mathbf{k}^{m+1}} \sum_{j=1}^{n_t} \sum_{i=1}^{n_j} \left(s^{m+1}_{\mathscr{K}_j(i)} - s^*_{i,j} \right)^2 \tag{3.12}$$

subject to:

$$\left(\mathbf{A}^m + \frac{1}{\Delta t_j} \mathbf{B} \right) \mathbf{s}_j^{m+1} = \frac{1}{\Delta t_j} \mathbf{B} \mathbf{s}_{j-1}^{m+1} + \mathbf{D}_j^m (\mathbf{k}^{m+1} - \mathbf{k}^m) + \mathbf{q},$$

$$\mathbf{k}_{\min} \leq \mathbf{k}^{m+1} \leq \mathbf{k}_{\max} \qquad\qquad j = 1, \ldots, n_t$$

We can consider convergence achieved if the change in conductivity is small, *i.e.*, $|\mathbf{k}^{m+1} - \mathbf{k}^m| < \tau$, where τ is a predefined tolerance, or if an insignificant change in the objective of equation (3.12) is observed. For convex programming problems, this process will converge to the global optimum of the original nonlinear inverse problem (Equation (3.5)). However, it is important to note that, in general, this algorithm only guarantees convergence to a local optimum for non-convex problems [5].

The algorithm presented thus far has not been used widely in practice due to the difficulty of solving each successive QP problem for real-world large-scale models. Depending on the QP algorithm employed, the successive QP problems (Equation (3.12)) can be highly computationally demanding and become impractical or even infeasible. Therefore, Gauss-Marquardt-Levenberg methods (*e.g.*, PEST [15] and UCODE [30]) have become more popular for solving inverse problems in groundwater flow. However, the linearization of the governing equations does, in fact, result in a linear model whose order (*i.e.*, number of equations) can be reduced significantly with the application of modern POD technology.

With a much smaller set of equations in the constraint set, the optimization problem (Equation (3.12)) can be solved very efficiently resulting in a more efficient and tractable overall estimation procedure.

3.3 Model Reduction via POD

In order to apply POD as accurately as possible to the linearized equations (Equation (3.9)), the natural system dynamics must be removed [39]. In other words, the model must be one in which the state variable remains at rest, *i.e.*, zero everywhere, unless some forcing is applied. This is naturally true for models of drawdown where the superposition principle is used to remove the natural system dynamics from the governing equations of groundwater flow. However, in the case of parameter estimation, we are not interested in optimizing pumping rates. Here we are interested in the manner in which drawdown changes given a change in the hydraulic conductivity distribution. Accordingly, we must develop a linearized model that relates changes in drawdown, δ_s, with changes in hydraulic conductivity, δ_k. This model must remain at rest, *i.e.*, $\delta_s = \mathbf{0}$, when there is no forcing, *i.e.*, $\delta_k = \mathbf{0}$. We obtain such a model by rewriting Equation (3.9), using the superposition principle, to yield

$$\mathbf{B}\frac{d\delta_s}{dt} = \mathbf{A}^m\delta_s + \mathbf{D}^m\delta_k, \tag{3.13}$$

where $\delta_s = \mathbf{s}^{m+1} - \mathbf{s}^m$ and $\delta_k = \mathbf{k}^{m+1} - \mathbf{k}^m$. This equation has the same general form as Equation (3.3); however, the state variable is now δ_s and the forcing term is now $\mathbf{D}^m\delta_k$. Hence, the linearized model relates changes in drawdown (δ_s) to perturbations in zonal hydraulic conductivity values (δ_k).

Since the linearized model has the same form as that in Equations (3.3) and Equation (2.3), POD can be applied using the same POD methodology outlined in Section 2.2. Namely,

the procedure listed at the end of Section 2.2.1 can be applied. With the natrual system dynamics removed, the model can be approximated as follows

$$\delta_s(t) \approx \hat{\delta}_s(t) = \sum_{i=1}^{n_s} \mathbf{u}_i \delta_{s_{r_i}}(t) = \mathbf{U}\delta_{s_r}(t) \tag{3.14}$$

where $\mathbf{U}$ is the $n \times n_s$ matrix of spatial basis functions that span the reduced model space and δ_{s_r} is the vector of weighting functions which is considered the state vector in the reduced model space. Equation (3.14) is similar to Equation (2.4) with a different state variable. The matrix $\mathbf{U}$ can be calculated via PCA as described previously. The snapshots are collected, normalized and formed as the columns of a matrix, $\mathbf{X}$. $\mathbf{U}$ is then calculated by solving the following eigenvalue problem,

$$\mathbf{X}\mathbf{X}^T = \mathbf{U}\Lambda\mathbf{U}^T \tag{3.15}$$

Based on the relative magnitude of the eigenvalues in Λ, basis functions within the matrix $\mathbf{U}$ are discarded (Equation (2.5)). The resulting matrix spans the reduced-model subspace and is analogous to the matrix $\mathbf{P}$ discussed previously.

Upon the application of the Galerkin Projection (Equation (2.8)), the reduced linearized model is written as follows

$$\tilde{\mathbf{B}}\frac{d\delta_{s_r}}{\partial t} = \tilde{\mathbf{A}}\delta_{s_r} + \tilde{\mathbf{D}}^m\delta_k \tag{3.16}$$

where $\tilde{\mathbf{B}} = \mathbf{P}^T\mathbf{B}\mathbf{P}$, $\tilde{\mathbf{A}}^m = \mathbf{P}^T\mathbf{A}^m\mathbf{P}$ and $\tilde{\mathbf{D}}^m = \mathbf{P}^T\mathbf{D}^m$

This reduced system of ODEs can be solved by any stable time stepping technique, such as Implicit Euler:

$$\left(\tilde{\mathbf{A}}^m + \frac{1}{\Delta t_j}\tilde{\mathbf{B}}\right)\delta_{s_{r_j}} = \frac{1}{\Delta t_j}\tilde{\mathbf{B}}\delta_{s_{r_{j-1}}} + \tilde{\mathbf{D}}_j^m\delta_k, \tag{3.17}$$

However, because of Equation (3.17)'s drastically reduced size ($n_p \ll n$), often by several orders of magnitude, the system also can be solved very efficiently by analytical methods via

matrix exponential [4, 41].

3.3.1 Reduced Order Quadratic Programming Formulation

The reduced linearized model now can be used to solve each successive quadratic programming problem. Noting that $s_{i,j}^{m+1} = s_{i,j}^{m} + \mathbf{p}_i^T \delta_{s_{r_j}}$, substituting Equation (3.17) into Equation (3.12) results in the following QP problem:

$$
\begin{aligned}
&\min_{\mathbf{k}^{m+1}} \sum_{j=1}^{n_t} \sum_{i=1}^{n_j} \left(\mathbf{p}_{\mathscr{K}_j(i)}^T \delta_{s_{r_j}} + s_{\mathscr{K}_j(i)}^{m} - s_{i,j}^{*} \right)^2 \\
&\quad \text{subject to:} \\
&\quad \left(\tilde{\mathbf{A}}^m + \frac{1}{\Delta t_j} \tilde{\mathbf{B}} \right) \delta_{s_{r_j}} = \frac{1}{\Delta t_j} \tilde{\mathbf{B}} \delta_{s_{r_{j-1}}} + \tilde{\mathbf{D}}_j^m \delta_k, \quad j = 1, \ldots, n_t \\
&\quad \delta_k = \mathbf{k}^{m+1} - \mathbf{k}^m \\
&\quad \mathbf{k}_{\min} \leq \mathbf{k}^{m+1} \leq \mathbf{k}_{\max}
\end{aligned}
\tag{3.18}
$$

where $\mathbf{p}_{\mathscr{K}_j(i)}$ is the $\mathscr{K}_j(i)$-th row of the $\mathbf{P}$ matrix. It is important to note that from one QP problem to the next (*i.e.*, between outer iterations of the overall algorithm) the principal vectors must be re-evaluated in order for the reduced model to achieve the greatest accuracy. This is a result of changing values of hydraulic conductivity between successive QPs (*i.e.*, $\mathbf{A}$ is a function of $\mathbf{k}$). However, as shown in this research, if the principal vectors are evaluated using a reasonable initial guess, subsequent inaccuracies produced by the reduced models throughout the algorithm become negligible. It is also important to note that the limitation on the number of parameters to be estimated is no different from that of a quadratic programming problem, which can be quite large.

3.4 One-Dimensional Test Case

In this section, the proposed method is applied to the one-dimensional test problem, illustrated in Figure 2.1, with the same properties and definitions as previously discussed. First, the performance of the POD model reduction methodology as applied to the linearized model (Equation (3.16)) is investigated. Figure 3.1 illustrates the solution to the original full model along with the results of both the linearized full model and linearized reduced model given a change of hydraulic conductivity in each zone of 1.0 m/d (the initial values are those displayed in Figure 2.1). For this test case, the errors between the linearized full model and the linearized reduced model are on the same order of magnitude as those shown for the one-dimensional original full model in Chapter 2 (Figure 2.2). One can, therefore, conclude that the solutions obtained from the linearized full model and the linearized reduced model are essentially identical.

The parameter estimation algorithm presented in this dissertation was applied to the one-dimensional test case. The algorithm was tested under three scenarios: (1) using the linearized full model only; (2) using POD model reduction of the linearized model where the reduced basis is updated at each iteration of the quasilinearization procedure; and (3) using POD model reduction for the linearized model without updating the reduced basis, *i.e.*, the reduced basis is determined using the initial values or the initial "guess" of hydraulic conductivity and never updated. A flow chart of the overall algorithm employed in this study is shown in Figure 3.2.

Observations of drawdown were generated using the true parameter values of $k_1 = 15.0$ m/d and $k_2 = 5.0$ m/d and recorded at each time step at nine locations (x =20, 30, 40, 45, 51, 56, 61, 71, 81 m). The observations were also corrupted with normally distributed random noise to test the effects of measurement noise. Ten snapshots were selected optimally using the exponential function described in Section 2.3.1. Figure 3.3 illustrates the convergence results for these three scenarios using an initial guess of $k_1 = 0.1$ m/d and $k_2 = 0.1$ m/d.

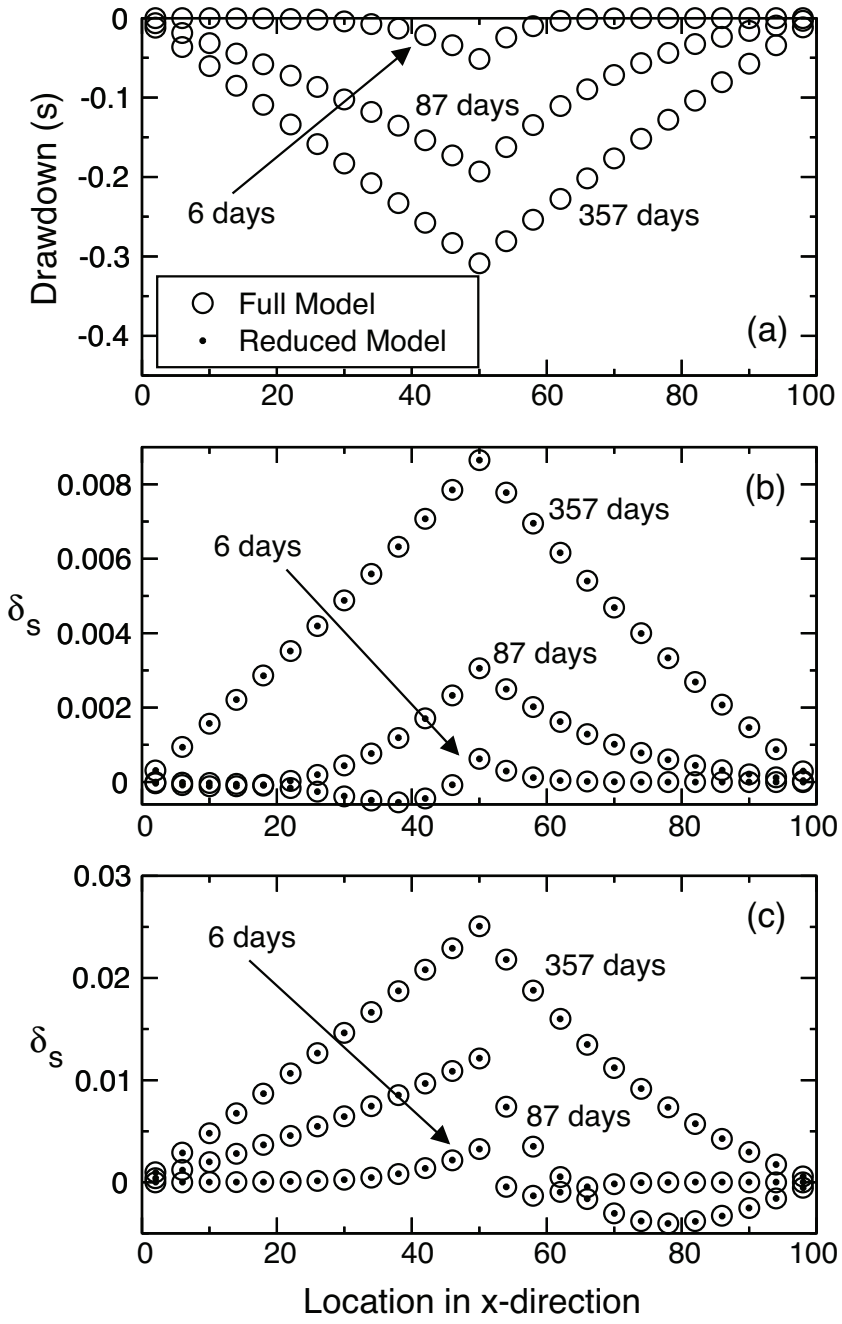

Figure 3.1: One-dimensional test model results for (a) the full, original flow model; (b) the linearized full and reduced models with k_1 increased by 1.0 m/d; and (c) the linearized full and reduced models with k_2 increased by 1.0 m/d.

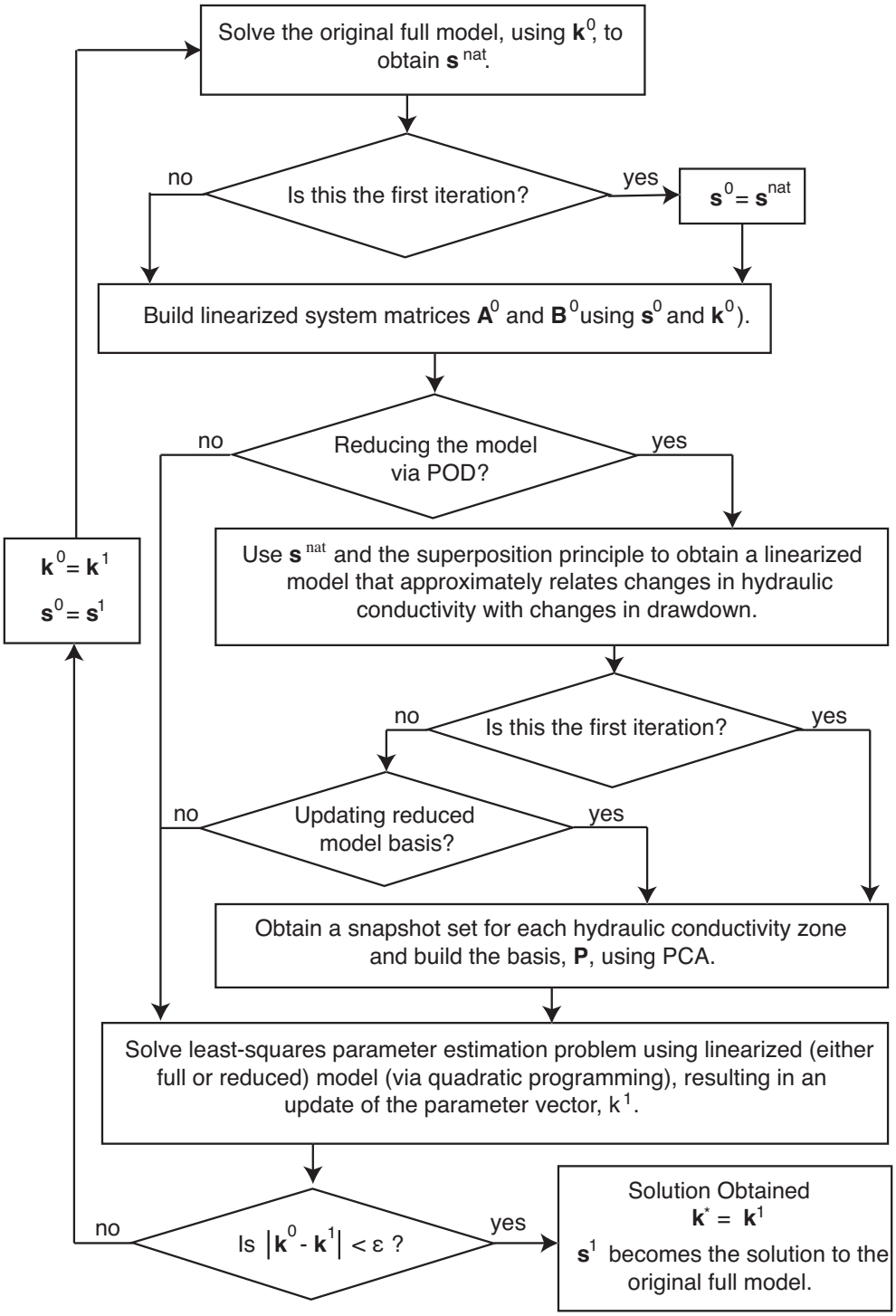

Figure 3.2: Flow chart of the algorithm presented in this study for all three scenarios.

The rate of convergence for the three scenarios was nearly identical until the least-squares objective had fallen below 10^{-6}. After this point, the algorithm using scenarios 1 and 2 proceeded to converge super-linearly, whereas the algorithm employing scenario 3 appeared to converge linearly. Significant differences in convergence rates between scenarios 1 and 2 were not observed until the least-squares objective was very small. However, if a different initial estimate of hydraulic conductivity were used, the relative rates of convergence for the three scenarios could be quite different; "good" initial guesses could result in very little difference in convergence between the three scenarios. In the case where measurement noise was added, there were negligible differences between the convergence rates of the three scenarios. This is due to the fact that errors associated with measurement noise dominated those associated with model order reduction via POD. Aside from convergence rates, it is also important to evaluate whether or not the algorithm actually converges (oscillatory behavior is possible for scenario 3) or if it converges to the global optimum. Table 3.1 lists convergence results for a series of initial estimates of hydraulic conductivity (without measurement noise); the algorithm was considered to have converged when the least-squares objective had fallen below 10^{-16} or diverged when more than 80 iterations were realized without convergence. The upper and lower bounds for each parameter were set to 10^{3} m/d and 10^{-8} m/d, respectively. Although scenario 3 has some potential for oscillation, the initial guess 382 must be very poor for non-convergence to occur. In all cases tested, including those listed in Table 3.1, the global optimum was achieved; however, this cannot be guaranteed in the presence of insensitive and/or correlated parameters.

3.5 Two-Dimensional Application: Oristano, Italy

The algorithm presented in this study was used to solve the inverse problem for a two-dimensional representation of a groundwater flow model in Oristano, Italy. The plain of

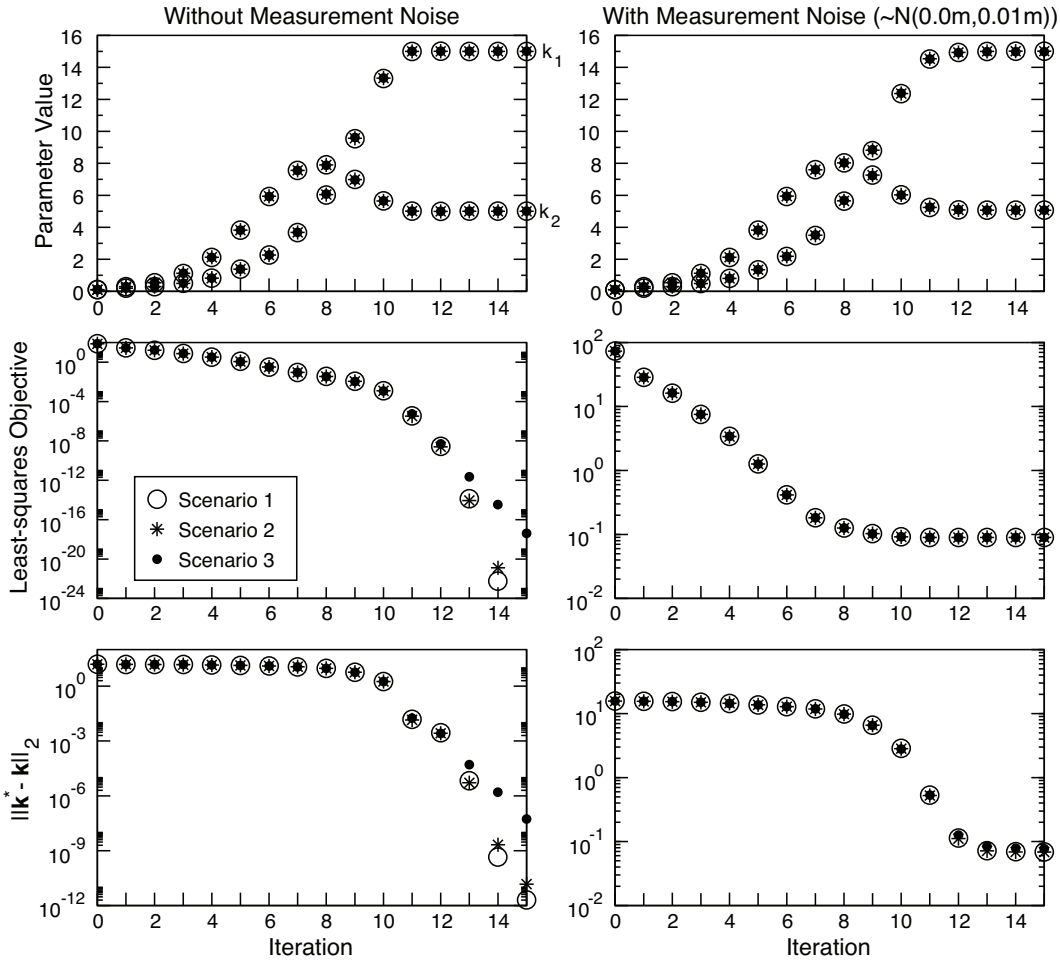

Figure 3.3: Convergence results for the one-dimensional test case, with and without measurement noise, using an initial estimate for hydraulic conductivity of $k_1 = 0.1$ m/d and $k_2 = 0.1$ m/d (note that the vertical scales may differ).

Table 3.1: Convergence statistics for the one-dimensional test case using various initial estimates of the parameters.

		Converge?			Iterations Required		
Initial Estimate		scenario:			scenario:		
k_1	k_2	1	2	3	1	2	3
0.1	0.1	yes	yes	yes	14	14	15
10	10	yes	yes	yes	6	6	6
17	17	yes	yes	yes	12	12	12
100	100	yes	yes	yes	18	18	16
0.15	50	yes	yes	no	16	16	–
50	0.15	yes	yes	yes	9	9	17

Oristano is located in west-central Sardinia. The morphology of the territory is predominantly flat surrounded by the Monti Ferru and the Monti Arci hills on the east and by the sea on the west. A heavily exploited multi-aquifer system provides the source of water for agricultural and industrial uses. Approximately 25,000 wells are estimated to exist in the study region, although the number of wells that are actively withdrawing water from the aquifer system for agricultural and industrial uses is not known. Of these, 500 wells (some located also in the confined aquifer) have been monitored during recent years. The thickness of the multi-aquifer system ranges from a minimum of $\sim$ 28 m close to the hills and a maximum of $\sim$ 218.5 m close to the sea. Three major units can be identified: a phreatic aquifer with average thickness of $\sim$ 12 m, a confining layer with an average thickness of $\sim$ 4 m, and a confined aquifer with an average thickness of $\sim$ 110 m [9]. The focus of this research was on the confined aquifer, where most of the groundwater withdrawals take place. Since the major objective of this research is to test the proposed algorithm for models with a large, realistic, number of computational nodes, synthetic, simplified data was assumed for pumping, recharge, and boundary conditions.

The numerical model for groundwater flow is discretized using the finite element method. The model contains 29,197 nodes and 57,888 elements and contains local grid refinement in 11 regions (Figure 3.4). For the purposes of this study, the model forcing was simplified such that there are six extraction well clusters (with a constant rate of 5,000 m^3/d each) and the entire outer boundary of the model is represented with Dirichlet boundary conditions (Figure 3.4). Specific storage is assumed constant throughout the model at 10^{-5} m^{-1}. Three different zonation patterns containing three, seven and 15 zones, respectively, were considered for hydraulic conductivity (Figure 3.5). The "true" values of hydraulic conductivity (*i.e.*, those used to generate the observations) are listed in Table 3.2 for each of the three zonation patterns. The initial values of each zone were set to 1.0 m/d. The same three algorithm scenarios used in the one-dimensional test case also were employed in the Oristano model.

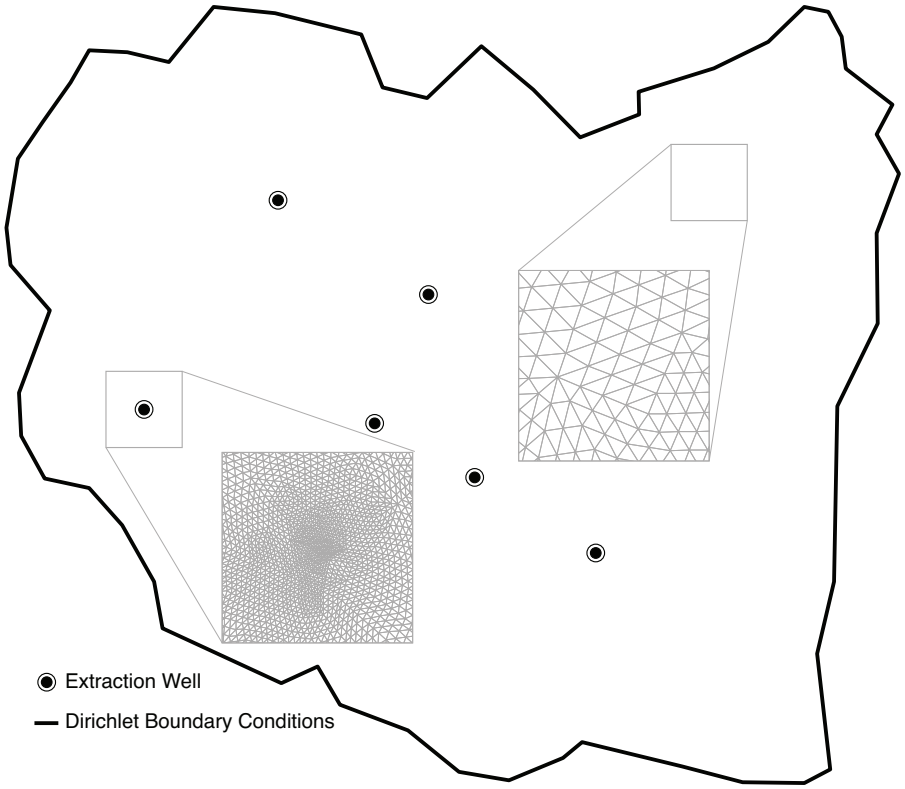

Figure 3.4: The model grid used as a two-dimensional "slice" of the Oristano, Italy, model.

Using the true parameter values, drawdown observations were generated at the locations shown in Figure 3.5 for each time step.

Figure 3.6 shows the comparison between the linearized full model and linearized reduced model for the three-zone hydraulic conductivity distribution (Figure 3.5). The differences between the linearized full and linearized reduced model are indistinguishable and differences at the locations of the wells (maximum drawdown) are usually less than 0.0001 m. The impact of changing the hydraulic conductivity value of a zone is largely dependent on whether or not significant forcing resides in that zone. For example, in Figure 3.6, changing the hydraulic conductivity in zone 1 resulted in large changes in drawdown at the locations of the wells within zone 1; the same is true for zones 2 and 3. The three scenarios listed in Section 3.4

Table 3.2: True values of hydraulic conductivity by zone for the three zonation patterns considered (m/d).

	Zonation Pattern		
Zone	3-zone	7-zone	15-zone
1	15.0	15.0	15.0
2	5.0	5.0	5.0
3	7.0	7.0	7.0
4		12.0	12.0
5		3.0	3.0
6		20.0	20.0
7		10.0	10.0
8			2.0
9			9.0
10			18.0
11			21.5
12			4.3
13			0.5
14			16.1
15			1.0

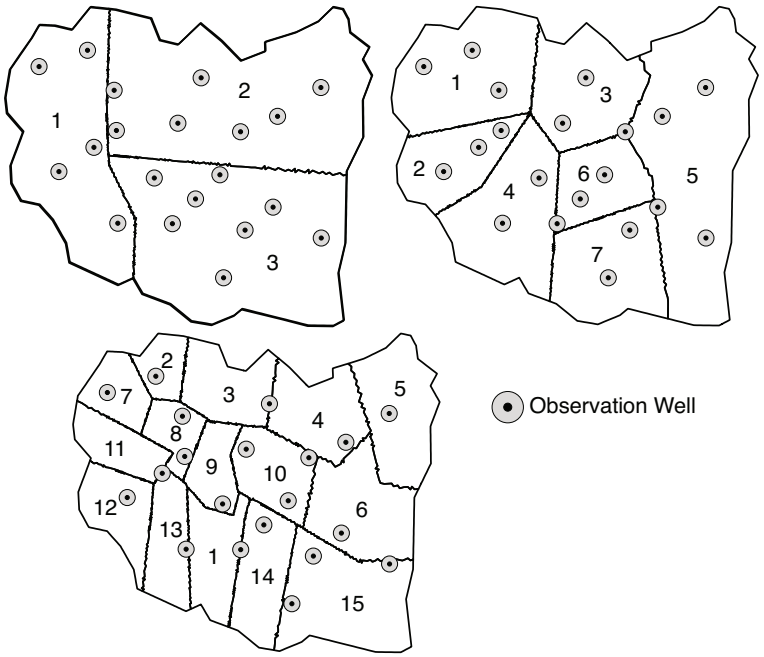

Figure 3.5: Zonation patterns used for the Oristano, Italy model.

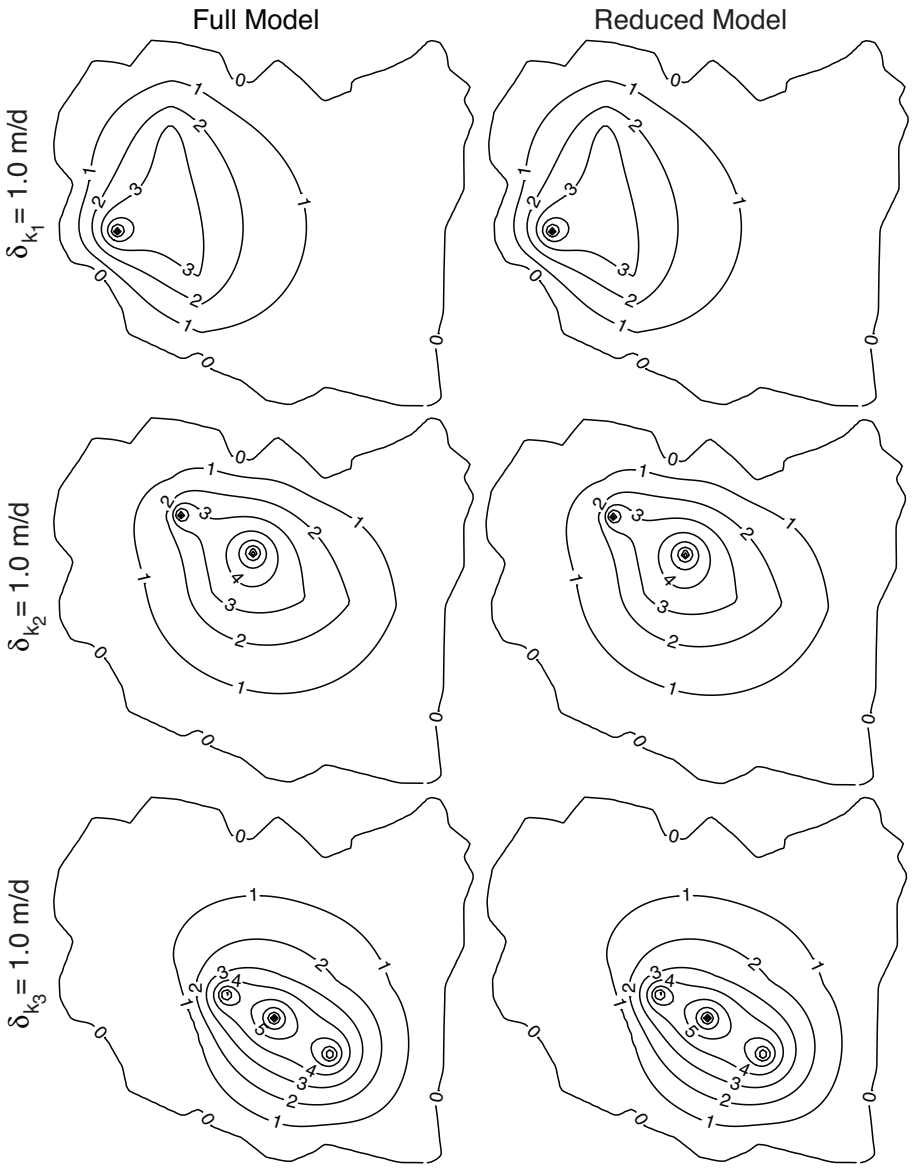

Figure 3.6: Changes in drawdown (m) given a unit change in hydraulic conductivity (1.0 m/d) for both the linearized full and reduced models.

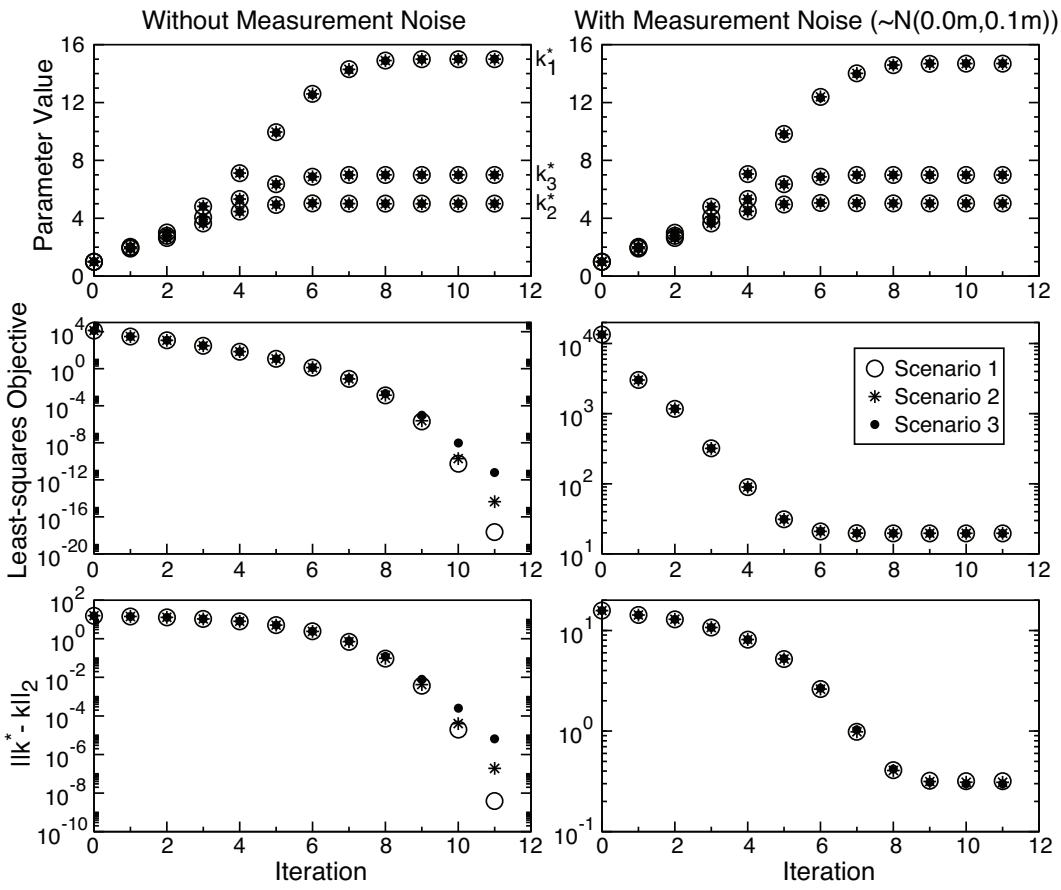

Figure 3.7: Convergence results for the 3-zone case with and without measurement noise.

were conducted for the Oristano model using the procedure outlined in Figure 3.2. The effects of measurement noise also were explored; random Gaussian noise ($\sim N(0.0\text{ m}, 0.1\text{ m})$) was added to the observation data. Figure 3.7 shows the convergence of the three-zone model with and without measurement noise. Similar to the convergence results of the one-dimensional test case, all three scenarios converge similarly (without noise) until the objective fell below 10^{-6}, where scenarios 2 and 3 began to deviate from scenario 1. However, with measurement noise, the least-squares objective cannot fall below approximately 20.0; therefore, there was no significant difference in convergence between the three scenarios. This is more realistic because, in practice, there always will be noise present in measured data.

The convergence results of the 7-zone and 15-zone models are shown in Figure 3.8. For

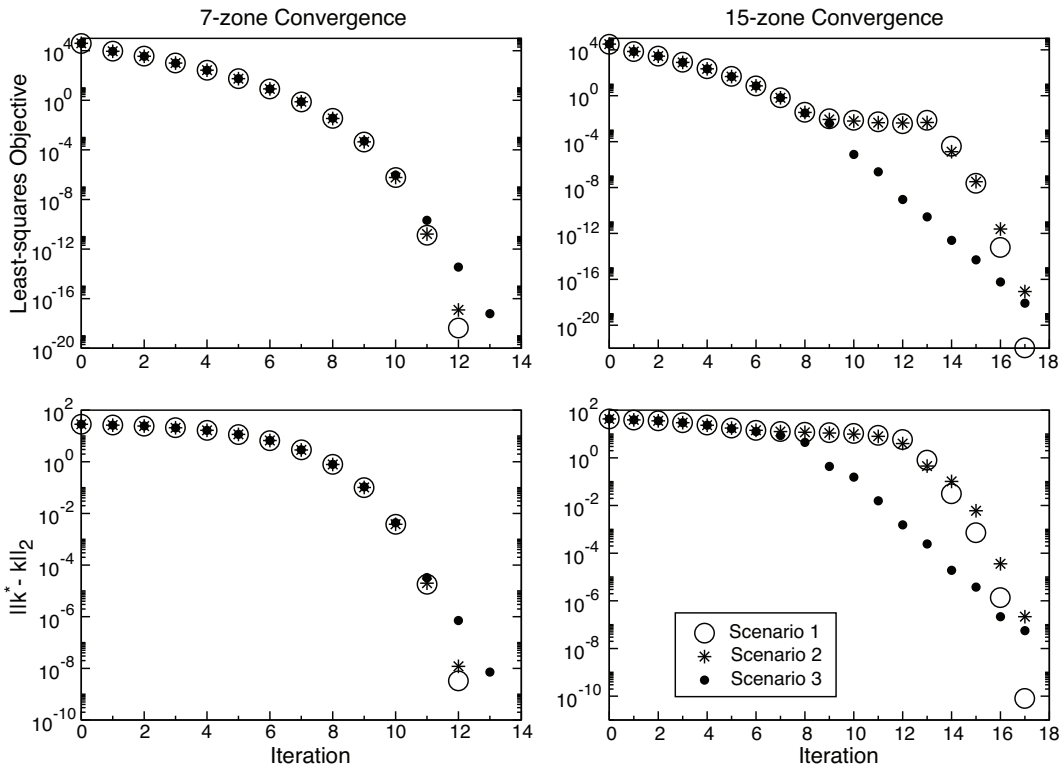

Figure 3.8: Convergence results for the 7 and 15-zone models.

the seven-zone case, the convergence of the three scenarios is similar to that of the three-zone Oristano model and the one-dimensional test model. However, the convergence of Scenarios 1 and 2 for the 15-zone case decreases around the fifth iteration. This is due to the fact that since the hydraulic conductivity of zone 7 is relatively insensitive to the least-squares objective, this value reaches its lower bound on the first iteration. Therefore, the remaining zonal values must be adjusted to "compensate" for this constraint. Furthermore, due to the insensitivity of zone 7, the impacts associated with the lower bound constraint are not noticeable until the ninth iteration, when the objective starts to become small. At this point, the algorithm convergence is reduced until the hydraulic conductivity of zone 7 gets close to the true value, after which super-linear convergence is obtained. The convergence of the hydraulic conductivities of zones 2, 3, and 7, as shown in Figure 3.9, confirms these observations.

The results associated with Scenario 3 do not demonstrate the same impacts on convergence resulting from the parameters being constrained by their lower bounds. This is likely due to the fact that the Jacobian matrices (Section 3.2.2) are projected onto a subspace that is determined using the initial guess of hydraulic conductivity, which does not contain parameters residing on their lower bounds, resulting in more robust or better-conditioned Jacobian matrices. This is not true for Scenario 2 because the basis functions, and hence the reduced-model subspace, are updated at each iteration using the current parameter values. So, at the second iteration, the basis functions are reconstructed using snapshots generated from a parameter set that is constrained by its lower bound. In summary, the results of Scenario 3 may indicate a potentially unforeseen advantage associated with the proposed algorithm, in addition to computational considerations (of which is the focus of this study), and is a subject of further research.

Comparing, quantitatively, the computational improvements associated with the proposed method is not straightforward. As shown previously, each scenario may require a different number of iterations to achieve convergence. Additionally, each scenario may arrive at different parameter values throughout the inverse problem, which, in turn, may lead to different computational costs associated with iterative QP solvers. However, some comparisons are required. The linearized full model for the 15-zone case, at iteration 1, required about 24.5 seconds of run time on an iMac quadcore computer with an INTEL 2.93 GHz i7 processor equipped with 12 GB RAM, 256 KB L2 cache (per core), 8 MB L3 cache, with no hyperthreading and no automatic parallelization using GNU GFortran compiler with O3 automatic optimization. The same simulation with the linearized reduced model required about 10.3 seconds. All 150 principal vectors were retained for this reduced-model simulation; truncation of principal vectors will yield drastic reductions in the reduced-model run time. The eigenvalue decomposition required very little effort (about 1.4 seconds). Solving the QP problem at iteration 1 using the linearized full and reduced versions of the quasilin-

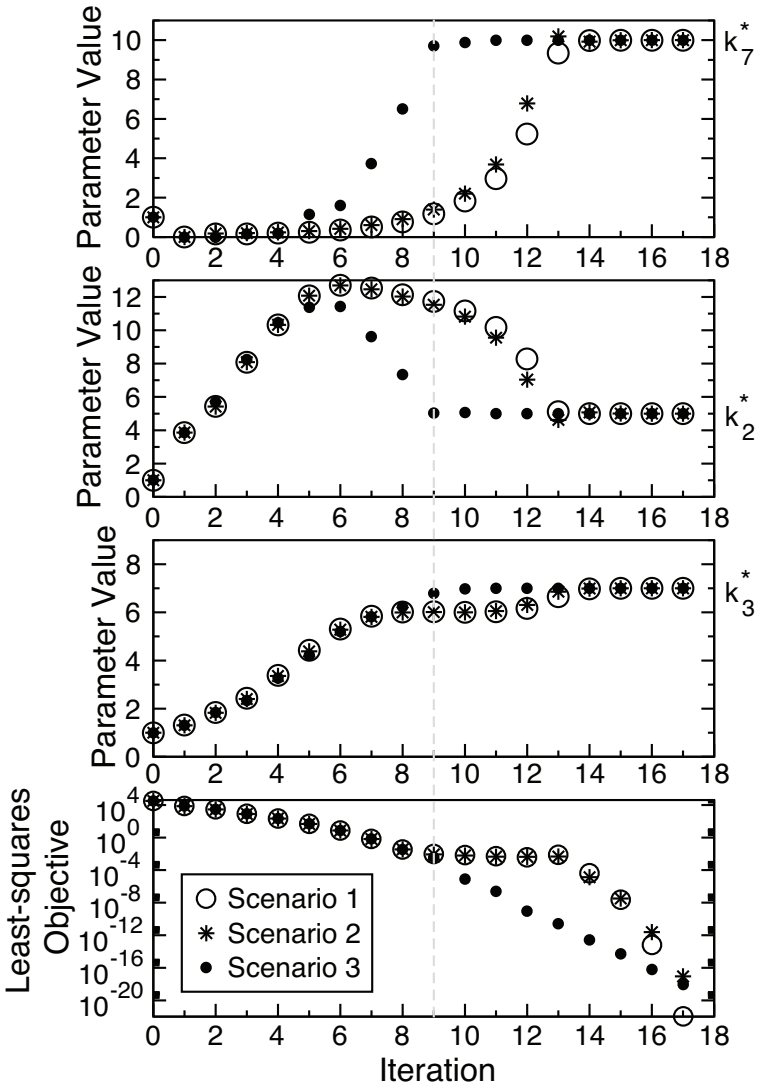

Figure 3.9: Convergence behavior of hydraulic conductivity in zones 2, 3 and 7 and the objective function for the 15-zone case. The dashed grey line indicates the iteration in which the objective function for Scenario 3 diverges from that of Scenarios 1 and 2.

earization procedure (not including snapshot generation) required 37.7 and 15.35 minutes, respectively. This comparison will be different for each iteration. The overall inverse problem (15 zone case) for Scenarios 1, 2 and 3 required 20 hours 13 minutes, 7 hours 12 minutes and 3 hours 51 minutes, respectively, yielding a speedup of more than 5 times for the method proposed in this study. Truncating principal vectors, exploiting the small size of the QPs, and more efficient data storage will likely reduce the computational expense even further.

Chapter 4

Discussion and Conclusions

The accuracy of a reduced model, developed via POD, depends strongly on the manner in which full-model snapshots are taken in time. A snapshot selection technique has been developed based on the fact that confined aquifers, subjected to constant pumping, reach approximate steady state conditions in an exponential manner. This exponential selection of snapshots assumes fixed initial and final snapshot times. Given a pre-selected fixed number of snapshots to be used in the POD procedure, the optimal snapshot times are determined by maximizing the smallest eigenvalue of the covariance matrix. This optimality criterion, similar to the E-optimality criterion used in experimental design, ensures that all the snapshots in the computed set are as significant as possible after the PCA phase of POD. The initial snap-shot is set small enough such that there is only a very slight change in drawdown from the initial conditions. The final snapshot is fixed at a time representative of approximate steady state conditions. A simple exponential function then defines the manner in which snapshots are selected in between these time steps. There are three parameters in this function; however, since the first and last snapshot is fixed, only one of the parameters needs to be optimized, *i.e.*, for a particular value of one parameter, the other two can be calculated.

Solving this problem of optimal snapshot selection for a large scale, real-world, problem can be computationally demanding. This would require a very fine temporal discretization, in which the details are not straight forward, and the solution must be recorded at each time step. Then the exponential selection method developed in this study can be applied. However, this method requires a search algorithm to determine the best parameter values in the exponential snapshot selection function. This process would have to be repeated for each well. In addition, this analysis would have to be conducted for each real-world model. However, the optimal parameters of the exponential formula, for any real-world model, are primarily a function of both the model parameters and model geometry. To approximate the optimal snapshot set for any domain shape and heterogeneous porous media, we have developed a simple protocol for snapshot selection based on the optimal snapshot set of a unit cubic domain and a dimensionless equation. Since we are looking at selecting snapshot times, we need to translate the dimensionless times into real-world times. The transformation from dimensionless time to real-world time is approximately linear and is based on the properties of the real-world model. The determination of the proportionality constant in this relationship is obtained as the ratio between the lengths of time in which approximate steady state conditions are reached for both the dimensionless and real-world models.

We have determined the optimal snapshot set for the dimensionless model in three dimensions by determining the appropriate parameter values in the exponential snapshot selection function via exhaustive search. The accuracy of the reduced model was assessed by evaluating the norm of the error between fullmodel and reducedmodel solutions. The results have shown that this technique yields an accurate reduced model. The optimal snapshot set was then used to evaluate the accuracy of a simple heterogeneous test problem defined on a regular domain, mimicking a realworld model. Pseudosteady state times allowed the determination of the transformation between the dimensionless and heterogeneous models. The results showed that the suboptimality of the resulting snapshot set does not significantly

influence the accuracy of the reduced model.

The applicability of the proposed snapshot selection approach was tested on a real aquifer model. The resulting optimal snapshot times for the dimensionless model were mapped to their equivalent times in a basin scale model of Central Veneto, Italy. This model consists of 222,687 nodes and 1,289,570 elements with more than 50 zones each containing different values for hydrogeologic properties. The reduced-model solution contains very small errors when compared to the full model, and achieved a reduction in CPU time of approximately 1000 times. The full-model system, with a single well, was reduced from 222,687 ODEs to 10 ODEs which can be reduced even further by omitting insignificant principal vectors from the basis spanning the reduced-model solution space. This result shows that the proposed methodology can be used very effectively for groundwater simulation models, in particular when repeated runs with different forcings or different parameter values are required, such as in the case of scenario evaluation, groundwater management models, Monte Carlo simulations, etc.

POD is a very effective tool for reducing the computational burden of groundwater simulations for linear problems, although its applicability and robustness in nonlinear cases is still debated and needs to be studied in more depth. Efficiency can be further enhanced using matrix exponentiation algorithms as opposed to time-stepping strategies. Matrix exponentiation schemes using, for example, Leja polynomials [6, 8] allow for the evaluation of the solution at selected times without the need to go through more commonly used time-stepping schemes. This will significantly aid in snapshot selection as it can provide the model solution at any specific time, thus alleviating problems associated with matching snapshot times with the time steps of a time-stepping strategy.

The computational burden associated with solving the problem of parameter estimation is dependent on both the number of times the model under investigation must be called as well as the computational expense associated with calling this model. A new technique has been

developed for solving the inverse problem in which the computational burden of solving the model is dramatically reduced. The method proposed is an extension of the quasilinearization technique where the governing system of differential equations is linearized with respect to the parameters, resulting in a least-squares regression problem or a quadratic programming (QP) problem. The solution becomes an update on the parameter set. This process is then repeated until convergence takes place. Applying the POD method drastically reduces the computational burden associated with these regression problems. This is achieved by reducing the dimensionality of the linearized flow model embedded in the QP problem to be solved at each iteration.

The proposed algorithm was used to solve the inverse problem for confined groundwater flow models. First, a one-dimensional test case was used to illustrate the algorithm mechanics. The methodology then was applied to a two-dimensional, finely discretized version of a real model in the Oristano region of the island of Sardinia, Italy. The results obtained from numerical experiments indicate that the convergence of the quasilinearization scheme was nearly identical for the linearized full model and the POD reduced model derived from the linearized full model. This suggests that the proposed method may be feasible for solving real world large-scale inverse problems.

The implications associated with the reduced basis updates also were explored. Through simulation, the results have shown that this basis, *i.e.*, the reduced model subspace, does not need to be updated between successive iterations of the quasilinearization procedure, so long as the initial estimate of the parameter values is within the region of convergence, which may be slightly smaller than that of the algorithm without POD model reduction. Removing the need for updating the basis between iterations drastically reduces the computational burden of solving the inverse problem since the snapshot set needs to be developed only once, at the first iteration. In other words, the algorithm proceeds by calling the linearized full model once per parameter at the first iteration only. Then the algorithm continues such that, at

each iteration, the original full model is called once and a reduced-order QP problem is solved.

Numerical experiments indicate that without updating the reduced basis between iterations, the parameter estimation process may even become more stable and efficient. For the 15-zone case of the Oristano model, one of the parameter values was constrained by its lower bound at the first iteration. This was likely a result of this parameter being insensitive to the observation data. As a result, only the reduced-order algorithm for which the reduced basis was not updated at every iteration continued to converge super-linearly. This is likely the result of the subspace projection being based on the initial estimate and not on a parameter vector containing a parameter at its lower bound. This phenomenon of added stability to the inverse problem is beyond the scope of this paper and is a topic of further research.

Chapter 5

Ongoing and Future Research

5.1 Reduced Order Experimental Design for Estimating Unknown Groundwater Forcing

This topic explores optimal observation well locations and sampling frequencies in order to estimate unknown groundwater extraction. POD is used to reduce the groundwater flow model, thus reducing the computation burden and data storage space associated with solving this problem for heavily discretized models. This reduced model can store a significant amount of system information in a much smaller reduced state vector.

Consider the following general nonlinear statistical model,

$$\mathbf{y} = \mathbf{M}(\mathbf{p}) + \varepsilon \approx \mathbf{J}_D\mathbf{p} + \varepsilon \tag{5.1}$$

where, $\mathbf{y}$ is the vector of model state outputs that correspond to observations of state (*e.g.*, hydraulic head) and $\mathbf{M}$ is a nonlinear operator mapping the parameter vector, $\mathbf{p}$, to model

outputs and can be approximated linearly with the Jacobian, $\mathbf{J}_D$. Along with the sensitivity equation method, the proposed approach can efficiently prepare the Jacobian matrix, $\mathbf{J}_D$, associated with some design network. It can be shown that the covariance matrix associated with the estimated parameter vector ($\hat{\mathbf{p}}$) can be written as follows,

$$\mathrm{Var}(\hat{\mathbf{p}}) = \sigma_\varepsilon^2 (\mathbf{J}_D^T \mathbf{J}_D)^{-1} \tag{5.2}$$

so long as the expected value of ε is $\mathbf{0}$ and the columns of $\mathbf{J}_D$ are linearly independent. The optimal design for an observation network is one that minimizes the norm of this covariance matrix [13]. If the norm used for this analysis is the trace, the optimal experimental design is known as A-optimality. If unknown pumping rates are the parameters to be estimated, the optimal experimental design will then satisfy the following,

$$\min_{\text{design}} \mathrm{tr}\left(\mathbf{J}_D^T \mathbf{J}_D\right)^{-1}; \quad [\mathbf{J}_D]_{i,j} = \frac{\partial h_{i,t}}{\partial Q_{j,\tau}} \tag{5.3}$$

where index i is associated with the observation well location, index j the pumping well location, index t the sampling time, and index τ the extraction stress period.

In the real-world, pump operation is based on the characteristics of the pump in question and is a function of the lift required to remove the water. Therefore, the extraction rates to be estimated are a function of the head in the system. As such, to estimate extraction rates, one would need to incorporate functions that represent the wells' operation; thus, the parameters to be estimated are the operational condition of the extraction wells, *e.g.*, energy usage, pump speed, etc. This leads to some nonlinearities associated with the information obtained from an observation network given different pumping distributions. However, the flow model itself is linear and superposition holds with respect to forcing terms. Therefore, a POD reduced model can replace the full model and only needs to be generated once, off-line,

for unit values of extraction at each well (see Section 2.2).

Since pumping distributions can be widely variable, one must conduct a robust experimental design procedure to account for all possible distributions that could exist. Therefore, one would need to solve a series of experimental design problems and evaluate the design that provides the most information for all possible pumping distributions. This can be carried out as a Monte Carlo type analysis and would require many executions of the simulation model. Hence, the application of POD for this type of problem will be quite beneficial.

A Generic Algorithm (GA) can be used to optimize the observation well locations and sampling frequencies for maximizing the associated collected information given some feasible pumping distribution. This is then repeated for each possible pumping distribution. This approach can be easily applied to the proposed Oristano, Italy groundwater aquifer system. One would need to study the relationship among the number of observation wells, observation well locations, sampling frequency, and the collected information for estimating unknown groundwater extraction. Furthermore, it is clear to see that the successful application of POD for this problem indicates that it can be successfully extended to a groundwater management problem, where the extraction rates (and hence the decision variables) are a function of the hydraulic head.

5.2 Reduced Order Predictive Uncertainty Analysis using the Null-Space Monte Carlo Method

Groundwater models are essential for making predictions associated with how an aquifer system will respond to anthropogenic factors. However, the accuracy and reliability of a model is predicated on both the observations of state obtained in the field as well as any expert knowledge associated with the hydrogeologic setting. Often, there are few observations avail-

able and the hydrogeology is relatively unknown. In these cases, groundwater models must be drastically simplified in order for the calibration process to be well-determined. Optimal parameter dimensionality has been explored by *Yeh and Yoon* [48], *Sun and Yeh* [34], *Sun and Yeh* [35] and *Chiu et al* [11].

The subsurface lithology and composition is very complex and in order for the model to produce accurate predictions, the parameterization must also be equally complex and known. However, adding this degree of complexity to the model without knowing the truth, will result in a great deal of uncertainty in the parameter values and cannot produce a more reliable prediction. However, with this complexity added, the overall model predictive uncertainty, given the uncertainty in the parameter values (*i.e.*, parameter error), can be quantitatively explored via Monte Carlo techniques. Each randomly generated parameter field becomes an initial value for the calibration process. Each calibration process will likely yield different optimal parameter values and hence different model predictions. Therefore, each member of the Monte Carlo ensemble calibrates the model, but produces a different prediction. This type of analysis is known as calibration-constrained Monte Carlo analysis.

Calibration-constrained Monte Carlo analyses can be computationally demanding as they require many (often thousands) of model calibrations. This computational burden can be reduced immensely using the Null-Space Monte Carlo method proposed by *Tonkin and Doherty* [37] which has become part of the parameter estimation software known as PEST [15]. The method proceeds as follows [37].

For nonlinear regression, the update direction for each iteration is formulated as

$$\Delta \mathbf{p} = \left(\mathbf{J}^T \mathbf{Q} \mathbf{J}\right)^{-1} \mathbf{J}^t \mathbf{Q} \mathbf{r} \tag{5.4}$$

where $\Delta \mathbf{p}$ is the $n_b \times 1$ parameter upgrade vector, $\mathbf{J}$ is the $n_b \times n_b$ Jacobian matrix of sensitivities of the parameters with respect to the model-simulated equivalents of the obser-

vations, $\mathbf{Q}$ is an $n_b \times n_b$ matrix of weights, and $\mathbf{r}$ is the residual vector [37]. However, if the model is over-parameterized, many parameters will have the same relative impact on the model-simulated equivalents of the observations, *i.e.*, many columns of $\mathbf{J}$ will have nearly the same "shape". These redundancies can be dealt with systematically by conducting a spectral decomposition of $\mathbf{J}^T\mathbf{Q}\mathbf{J}$,

$$\mathbf{J}^T\mathbf{Q}\mathbf{J} = \mathbf{V}\mathbf{E}\mathbf{V}^T = \begin{bmatrix} \mathbf{V}_1 & \mathbf{V}_2 \end{bmatrix} \begin{bmatrix} \mathbf{E}_1 & \mathbf{0} \\ \mathbf{0} & \mathbf{E}_2 \end{bmatrix} \begin{bmatrix} \mathbf{V}_1 & \mathbf{V}_2 \end{bmatrix}^T \approx \mathbf{V_1}\mathbf{E}_1\mathbf{V}_1^T \tag{5.5}$$

where $\mathbf{E}_1$ is a diagonal matrix of eigenvalues considered to be statistically significant, $\mathbf{E}_2$ is a diagonal matrix of zero or near zero eigenvalues, $\mathbf{V}_1$ and $\mathbf{V}_2$ are matrices of orthonormal eigenvectors associated with $\mathbf{E}_1$ and $\mathbf{E}_2$, respectively. $\mathbf{V}_1$ is said to be a basis spanning the "calibration solution space" and $\mathbf{V}_2$ is a basis spanning the "calibration null space" [15]. Therefore, the calibration search direction can be approximated as follows

$$\Delta\mathbf{p} \approx \left(\mathbf{V}_1\mathbf{E}_1\mathbf{V}_1^T\right)^{-1}\mathbf{J}^t\mathbf{Q}\mathbf{r} \tag{5.6}$$

However, consider the projection of the upgrade vector in the direction of $\mathbf{V}$ which is equivalent to shifting and rotating the parameter coordinate system [36],

$$\Delta\mathbf{p} = \Delta\mathbf{V}\mathbf{p}_s \approx \Delta\mathbf{V}_1\mathbf{p}_s \tag{5.7}$$

The inverse problem now becomes one in which the objective is to search for a $\Delta\mathbf{p}_s$ $(n_k \times 1)$ that minimizes the least-squares objective [36] where k is the truncation level determined in Equation (5.5). Therefore, the problem is re-formulated in terms of estimating $\mathbf{p}_s$ which are

known as superparameters. Similarly, $\Delta \mathbf{p}_s$ is calculated as

$$\Delta \mathbf{p}_s = \left(\mathbf{J}_s^T \mathbf{Q} \mathbf{J}_s\right)^{-1} \mathbf{J}_s^t \mathbf{Q} \mathbf{r} \tag{5.8}$$

where, $\mathbf{J}_s$ is the $n_k \times n_k$ Jacobian matrix sensitivities of the superparameters with respect to the model-simulated equivalents of the observations. Note that $n_k \ll n_b$, thereby reducing the computational effort of the inverse problem as well as converting an over-parameterized under-determined inverse problem into a well-determined problem in which the superparameters can be uniquely identified. However, the basis $\mathbf{V}_1$ is determined based on the starting parameter values and never changes throughout the inverse problem.

This method, known as Truncated Singular Value Decomposition (TVSD) is solved in PEST using the Gauss-Levenberg-Marquardt method. However, the projection of Equation (5.7) can be thought of as an additional "level" of parameterization. Therefore, the reduced order parameter estimation procedure proposed in this dissertation is capable of solving this inverse problem. This is done by simply calculating $\mathbf{V}_1$ as in Equation (5.5) and rewriting Equation (3.16) as

$$\tilde{\mathbf{B}} \frac{d\delta_{s_r}}{\partial t} = \tilde{\mathbf{A}} \delta_{s_r} + \tilde{\mathbf{D}}^m \delta_{k_s} \tag{5.9}$$

where $\delta_{k_s} = \mathbf{V}_1(\mathbf{k}_s^{m+1} - \mathbf{k}_s^m)$. Then, solve the inverse problem using the proposed reduced order method for the superparameters, $\mathbf{k}_s$.

In addition to having defined a "calibration solution space" the TVSD method also defines the "calibration null space". It is in this null space that the majority of the parameter uncertainty and hence model predictive uncertainty resides. Therefore, random perturbations of the parameter values in a Monte Carlo framework can be projected into the calibration null space as follows [37],

$$(\mathbf{p} - \mathbf{p}_{\text{rand}})' = \mathbf{V}_2 \mathbf{V}_2^T (\mathbf{p} - \mathbf{p}_{\text{rand}}) \tag{5.10}$$

These perturbations are then added to the current calibrated parameters. If the model is linear, these randomly generated parameter values would exactly calibrate the model. However, since in groundwater flow, the parameter estimation process is nonlinear, these random parameter values may not calibrate the model. They are likely to be close enough that the corresponding inverse solution can be achieved in a small number of iterations of the calibration method used. However, for highly nonlinear models, several iterations of the calibration method will be required, which can be computationally expensive in the Monte Carlo framework. Currently, those who employ the Null-Space Monte Carlo method usually drop random realizations of the parameter vector if they do not converge in one or two iterations. However, if the Gauss-Levenberge-Marquardt algorithm in PEST can be replaced with the reduced order method proposed in this dissertation, the computational effort of conducting the Null-Space Monte Carlo method can be greatly reduced without the need to discard random realizations of the parameter vector. This would be a great contribution to model predictive uncertainty analysis.

5.3 Unconfined Groundwater Model Reduction via Proper Orthogonal Decomposition

The problem of artificial-recharge operations for groundwater systems has been extremely important in desert regions throughout California. These systems must be managed effectively where the objective could be, for example, to achieve desired water levels throughout the system while minimizing operational costs. The decision variables associated with this problem can include pond size, location, stage, etc., as well as some additional decision variables such as extraction/injection rates at wells. Solving this problem would require many model solutions subject to various values of the decision variables. Therefore, reducing the

computational burden associated with running the groundwater flow model will provide a significant benefit for solving this problem.

In order to evaluate the impacts of artificial recharge on a groundwater system, the uppermost layer of the model must be an unconfined layer with a water table condition. The governing equation for unconfined groundwater flow is as follows [3],

$$\nabla \cdot (Kh\nabla h) - q - S_y \frac{\partial h}{\partial t} = 0 \tag{5.11}$$

where S_y is the specific yield. Upon spatial discretization via finite differences, Equation (5.11) can be approximated as the following system of ordinary differential equations (ODEs)

$$\mathbf{B}\frac{d\mathbf{h}}{dt} + \mathbf{A}(\mathbf{h})\mathbf{h} - \mathbf{q} = \mathbf{0} \tag{5.12}$$

Equation (5.12) is similar to Equation (2.3) with state variable being hydraulic head and the stiffness matrix, $\mathbf{A}$, is now a function of the hydraulic head distribution. Therefore, Equation (5.12) is nonlinear with an approximately quadratic relationship between changes in forcing and changes in hydraulic head. As a result, iterative nonlinear solvers must be employed to solve this system. For example, MODFLOW uses a standard Picard iteration to solve for unconfined aquifers [17]. This method assumes an initial guess for head, $\mathbf{h}^0$, which is used to form the $\mathbf{A}(\mathbf{h})$ matrix as $\mathbf{A}(\mathbf{h}^0)$. The system is then solved as a linear system for $\mathbf{h}$. If the difference between $\mathbf{h}^0$ and $\mathbf{h}$ is larger than some tolerance, $\mathbf{h}^0$ is set equal to $\mathbf{h}$ and the process is repeated. This continues until convergence is achieved.

The use of POD for unconfined aquifers can be quite beneficial and needs to be explored. Complications may arise due to the nonlinear relationship between forcing and hydraulic head. However, at each Picard iteration, a "known" head distribution is used to determine the system matrices resulting in a linear system of ODEs. Therefore, superposition is now

upheld and the reduced model can return an accurate solution, given that the reduced basis $\mathbf{P}$ is accurate. Hence, the success of this approach depends on the ability of the basis $\mathbf{P}$ to produce an accurate reduced model over all possible distributions of hydraulic head, *i.e.*, all possible values of $\mathbf{h}^0$. The range of possible $\mathbf{h}^0$ values is predicated on the possible (or feasible) combinations of forcings that could exist. Therefore, one could explore snapshot selection using the Greedy Algorithm [7, 22] by addressing the forcing distribution as though it were a parameter to be estimated. This could potentially produce a robust $\mathbf{P}$ matrix for this type of problem as it has been shown in the literature to provide robust $\mathbf{P}$ matrices for capturing the variability of model parameters.

Bibliography

[1] Âli Y. Orbak, Esref Eskinat, and Osman S. Turkay. Physical parameter sensitivity of system eigenvalues and physical model reduction. *Journal of the Franklin Institute*, 341:631–655, 2004.

[2] Domenico A. Baú and Alex S. Mayer. Stochastic management of pump-and-treat strategies using surrogate functions. *Advances in Water Resources*, 29:1901–1917, 2006.

[3] Jacob Bear. *Hydraulics of Groundwater*. McGraw-Hill Inc., 1979.

[4] Richard E. Bellman. *Introduction to Matrix Analysis*. McGraw-Hill Inc., New York, NY, 1960.

[5] Richard E. Bellman. *Quasilinearization and Nonlinear Boundary-Value Problems*. Elsevier, New York, NY, 1965.

[6] L. Bergamaschi and M. Vianello. Efficient computation of the exponential operator for large, sparse, symmetric matrices. *Numerical Linear Algebra with Applications*, 7(1):27–45, 2000.

[7] T. Bui-Thanh, K. Willcox, and O. Ghattas. Model reduction for large-scale systems with high-dimensional parametric input space. *SIAM Journal of Scientific Computing*, 30:3270–3288, 2008.

[8] M. Caliari, M. Vianello, and L. Bergamaschi. Interpolating discrete advection-diffusion propagators at spectral leja sequences. *Journal of Computational and Applied Mathematics*, 172(1):79–99, 2004.

[9] P. L. Cau, G. Lecca, M. Putti, and C. Paniconi. The influence of a confining layer on saltwater intrusion and surface recharge and groundwater extraction conditions. *Computational Methods in Water Resources, Developments in Water Resources*, 47:493–500, 2002. edited by Hassanizadeh et al. Elsevier, Amsterdam.

[10] W. Cazemier, R.W.C.P. Verstappen, and A.E.P. Veldman. Proper orthogonal decomposition and low-dimensional models for driven cavity flows. *Physics of Fluids*, 10(7):1685–1699, 1998.

[11] Y-C. Chiu, N-Z. Sun, T. Nishikawa, and W. W-G. Yeh. Development of an objective-oriented groundwater model for conjunctive-use planning of surface water and groundwater. *Water Resources Research*, 45, 2009.

[12] Moody T. Chu. Inverse eigenvalue problems. *SIAM Rev.*, 40(1):1–39, 1998.

[13] Theodore G. Cleveland and William W-G. Yeh. Sampling network design for transport parameter identification. *Journal of Water Resources Planning and Management*, 116(6):764–783, 1990.

[14] R. L. Cooley. A comparison of several methods of solving nonlinear regression groundwater flow problems. *Water Resources Research*, 21(10):1525–1538, 1985.

[15] John Doherty. *PEST: Model-independent parameter estimation.* Watermark Numerical Computing, Brisbane, Queensland, Australia, 2010.

[16] G. Gambolati, M. Putti, and C. Paniconi. Three-dimensional model of coupled densitydependent flow and miscible salt transport in groundwater. *Seawater Intrusion in*

Coastal Aquifers: Concepts, Methods, and Practices, pages 315–362, 1999. Edited by J. Bear et al. Kluwer Academic, Dordrecht, Netherlands.

[17] A.W. Harbaugh, E.R. Banta, M.C. Hill, and M.G. McDonald. U.S. Geological Survey modular ground-water model - user guide to modularization concepts and the ground-water flow process. *U.S. Geolgical Survey Open File Report*, 00-92, 2000.

[18] Mary C. Hill and C. R. Tiedeman. *Effective Groundwater Model Calibration: With Analysis of Data, Sensitivities, Predictions, and Uncertainty*. Wiley-Interscience, Hoboken, N. J., 2007.

[19] Fritz John. *Partial Differential Equations*. Springer-Verlag, 4 edition, 1982.

[20] Marc E. Kowalski and Jian-Ming Jin. Model-order reduction of nonlinear models of electromagnetic phased-array hyperthermia. *IEEE Trans. on Biomedical Engineering*, 50(11):1243–1254, 2003.

[21] K. Levenberg. A method for the solution of certain non-linear problems in least squares. *Quarterly Journal of Applied Mathematics*, 2:164–168, 1944.

[22] C. Lieberman, K. Willcox, and O. Ghattas. Parameter and state model reduction for large-scale statistical inverse problems. *SIAM Journal of Scientific Computing*, 32(5):2523–2542, 2010.

[23] Micheal Loève. *Probability Theory*, volume 2. Springer-Verlag, 1978.

[24] D. W. Marquardt. An algorithm for least-squares estimation of nonlinear parameters. *Journal of the Society of Industrial and Applied Mathematics*, 11(2):431–441, 1963.

[25] James McPhee and William W-G. Yeh. Groundwater management using model reduction via empirical orthogonal functions. *Journal of Water Resources Planning and Management*, 134(2):161–170, 2008.

[26] Slobodan Mijalković. Using frequency response coherent structures for model-order reduction in microwave applications. *IEEE Trans. on Microwave Theory and Techniques*, 52(9):2292–2297, 2002.

[27] D. S. Oliver and Y. Chen. Recent progress on reservoir history matching: a review. *Computational Geophysics*, 15(1), 2011.

[28] H. M. Park, T. H. Kim, and D. H. Cho. Estimation of parameters in flow reactors using the karhunen-loève decomposition. *Computers and Chemical Engineering*, 23:109–123, 1998.

[29] G. M. Passadore, M. Monego, M. Sartori, M. Putti, L. Altissimo, A. Sottani, and A. Rinaldo. 3d flow model of aquifer systems of central veneto (italy). *2007 IAHR Congress Proceedings: Venice, Italy [CDROM]*, 2007. Edited by G. Di Silvio and S. Lanzoni. CORILA, Venice, Italy.

[30] E. C. Poeter, M. C. Hill, E. R. Banta, S. Mehl, and S. Christensen. *UCODE_2005 and Six Other Computer Codes for Universal Sensitivity Analysis, Calibration, and Uncertainty Evaluation:*. U.S. Geological Survey Techniques and Methods 6-A11, Reston, VA, 2005.

[31] Leah L. Rogers and Farid U. Dowla. Optimization of groundwater remediation using artificial neural networks with parallel solute transport modeling. *Water Resources Research*, 30(2):457–481, 1994.

[32] L. Sirovich. Turbulence and the dynamics of coherent structures. part 1: Coherent structures. *Quarterly of Applied Mathematics*, 45(3):561–571, 1987.

[33] Ne-Zheng Sun. *Theory and Applications of Transport in Prorous Media: Inverse Problems in Groundwater Modeling*. Kluwer Academic Publishers, 1994.

[34] Ne-Zheng Sun and William W-G. Yeh. Identification of parameter structure in groundwater inverse problem. *Water Resources Research*, 21(6):869–883, 1985.

[35] Ne-Zheng Sun and William W-G. Yeh. Development of objective-oriented groundwater models: 1. robust parameter identification. *Water Resources Research*, 43, 2007.

[36] M. Tonkin and J. Doherty. A hybrid regularized inversion methodology for highly parameterized environmental models. *Water Resources Research*, 41, 2005.

[37] M. Tonkin and J. Doherty. Calibration-constrained monte carlo analysis of highly parameterized models using subspace techniques. *Water Resources Research*, 45, 2009.

[38] P.T.M. Vermeulen, A.W. Heemick, and J.R. Valstar. Inverse modeling of groundwater flow using model reduction. *Water Resources Research*, 41, 2005.

[39] P.T.M. Vermeulen, A.W. Heemink, and C. T. Stroet. Reduced models for linear groundwater flow models using empirical orthogonal functions. *Advances in Water Resources*, 27:57–69, 2004.

[40] K. Willcox and J. Peraire. Balanced model reduction via the proper orthogonal decomposition. *AIAA Journal*, 40(11):2323–2330, 2002.

[41] R. Willis. A planning model for the management of groundwater quality. *Water Resources Research*, 15(6):1305–1312, 1979.

[42] Shengquan Yan and Barbara Minsker. Optimal groundwater remediation design using an adaptive neural network genetic algorithm. *Water Resources Research*, 42, 2006.

[43] William W-G. Yeh. Optimal identification of parameters in an inhomogeneous medium with quadratic programming. *Society of Petroleum Engineers Journal*, 15(5):371–375, 1975.

[44] William W-G. Yeh. Review of parameter identification procedures in groundwater hydrology: The inverse problem. *Water Resources Research*, 22(2):95–108, 1986.

[45] William W-G. Yeh. Systems analysis in ground-water planning and management. *Journal of Water Resources Planning and Management*, 118(3):224–237, 1992.

[46] William W-G. Yeh and G. W. Tauxe. Optimal identification aquifer diffusivity using quasilinearization. *Water Resources Research*, 7(4):955–962, 1971.

[47] William W-G. Yeh and G. W. Tauxe. Quasilinearization and the identification of aquifer parameters. *Water Resources Research*, 7(2):375–381, 1971.

[48] William W-G. Yeh and Y. S. Yoon. Aquifer parameter identification with optimum dimension in parameterization. *Water Resources Research*, 17(3):664–672, 1981.

[49] Weihua Zhang and Bernd Michaelis. Shape control with Karhunen-Loève-Decomposition: Theory and experimental results. *Journal of Intelligent Material Systems and Structures*, 14(7):415–422, 2003.